STUDIES ON PHOTOCHEMICAL VAPOR GENERATION OF SELENIUM

A THESIS SUBMITTED TO
THE GRADUATE SCHOOL OF NATURAL AND APPLIED SCIENCES
OF
MIDDLE EAST TECHNICAL UNIVERSITY

BY

MELİS ÇETMELİ

IN PARTIAL FULFILLMENT OF THE REQUIREMENTS
FOR
THE DEGREE OF MASTER OF SCIENCE
IN
CHEMISTRY

SEPTEMBER 2019

Approval of the thesis:

STUDIES ON PHOTOCHEMICAL VAPOR GENERATION OF SELENIUM

submitted by MELİS ÇETMELİ in partial fulfillment of the requirements for the degree of **Master of Science in Chemistry Department, Middle East Technical University** by,

Prof. Dr. Halil Kalıpçılar
Dean, Graduate School of **Natural and Applied Sciences** _____

Prof. Dr. Cihangir Tanyeli
Head of Department, **Chemistry** _____

Assoc. Prof. Dr. Gülay Ertaş
Supervisor, **Chemistry, METU** _____

Examining Committee Members:

Prof. Dr. Mürvet Volkan
Chemistry, METU _____

Assoc. Prof. Dr. Gülay Ertaş
Chemistry, METU _____

Prof. Dr. Ahmet M. Önal
Chemistry, METU _____

Assoc. Prof. Dr. Murat Kaya
Chemical Engineering and Applied Chemistry, Atılım University _____

Assist. Prof. Dr. Süreyya Özcan Kabasakal
Chemistry, METU _____

Date: 13.09.2019

I hereby declare that all information in this document has been obtained and presented in accordance with academic rules and ethical conduct. I also declare that, as required by these rules and conduct, I have fully cited and referenced all material and results that are not original to this work.

Name, Surname: Melis Çetmeli

Signature:

ABSTRACT

STUDIES ON PHOTOCHEMICAL VAPOR GENERATION OF SELENIUM

Çetmeli, Melis
Master of Science, Chemistry
Supervisor: Assoc. Prof. Dr. Gülay Ertaş

September 2019, 81 pages

Selenium is a significant trace element for human health. Selenium can be essential or toxic for human body depending on its concentration. Within the scope of this thesis, photochemical vapor generation tungsten coil atomization technique has been studied for the determination of selenium.

Volatile selenium compounds were generated by exposure of UV light of the solution containing selenium and acetic acid. To increase sensitivity of photochemical vapor generation system, the technique was combined with tungsten-coil atomization. Generated volatile selenium species were trapped and atomized on the rhodium coated tungsten coil. Among Ru, Rh, Ir, Co and Pd coated tungsten coils, selenium signal was sharper, more reproducible and more sensitive with rhodium coated tungsten coil.

The experimental parameters were optimized. LOD and LOQ of the technique were determined as 3.3 and 11.1 μg/L respectively.

Technique was applied to selenium dietary supplements containing sodium selenite. The concentration of selenium in tablets was determined by using photochemical vapor generation tungsten-coil atomization method. The result is consistent with the certificate value given by the company.

Interference from PVG-amenable elements, transition metals and earth base elements was investigated. The most severe interference effect on the signal of Se (IV) was observed from copper.

Keywords: Selenium, Photochemical Vapor Generation, Trapping, Atomic Absorption Spectrometry

ÖZ

FOTOKİMYASAL BUHAR OLUŞTURMA YÖNTEMİ İLE SELENYUM TAYİNİ ÇALIŞMALARI

Çetmeli, Melis
Yüksek Lisans, Kimya
Tez Danışmanı: Doç. Dr. Gülay Ertaş

Eylül 2019, 81 sayfa

Selenyum, insan sağlığı açısından çok önemli bir eser elementtir. Vücut için zaruri bir element olması veya toksik etki yaratması vücuttaki derişimine bağlı olarak değişkenlik gösterebilmektedir. Bu tez kapsamında, fotokimyasal buhar oluşturma tungsten bobin atomizasyon tekniği kullanılarak selenyum tayini çalışılmıştır.

Selenyum ve asetik asit içeren çözelti, UV ışığına maruz bırakılarak uçucu selenyum bileşikleri takip edilmiştir. Fotokimyasal buhar oluşturma sisteminin duyarlılığını artırmak için, teknik tungsten-bobini atomizasyonu ile birleştirilerek uçucu selenyum türleri tungsten bobini üzerinde tuzaklandı ve sonrasında atomize edildi. Ru, Rh, Ir, Co ve Pd kaplı tungsten bobinleri arasında, rodyum kaplama ile selenyum sinyalleri diğer kaplamalara göre daha keskin, tekrarlanabilir ve duyarlı olduğu tespit edildi.

Deneysel parametreler optimize edildi ve optimize koşullarda yapılan deneylerde tespit sınırı (LOD) ve tayin sınırı (LOQ) sırasıyla 3.3 and 11.1 μg/L olarak belirlendi.

PVG tekniği ile bu çalışma kapsamında sodyum selenit içeren selenyum takviye ürünlerine uygulanmıştır. Tabletlerde bulunan selenyum miktarı fotokimyasal buhar oluşturma tungsten-bobin atomizasyon yöntemi kullanılarak sertifika değerine uyumlu bir sonuç tespit edilmiştir.

Geliştirilen metodun; PVG'ye yatkın elementler, geçiş metalleri ve toprak temelli elementlerden kaynaklanabilecek olası girişim etkileri çalışılmıştır. En fazla girişim yapan elementin bakır olduğu gözlenmiştir.

Anahtar Kelimeler: Selenyum, Fotokimyasal Buhar Oluşturma, Tuzaklama, Atomik Absorpsiyon Spektrometre

To my family

ACKNOWLEDGEMENTS

I would like to express my gratitude to my supervisor Assoc. Prof. Dr. Gülay Ertaş for her guidance and support throughout this study. Thanks to her experience and analytical way of thinking, I learned many things.

I would like to thank Prof. Dr. Osman Yavuz Ataman for sharing his valuable knowledge with me throughout the study.

I would like to thank my lab mates: Canan Höçük, Sezin Atıcı Özdemir, Erhan Özdemir and Mehmet Bilgi Er not only for their help and support but also their valuable friendship. I also thank to C-50 members: Dr. Yeliz Akpınar, Begüm Avcı, Merve Nur Güven, Pakizan Tasman and Zuhal Selvi Vanlı for their help and friendship. They were all there for me whenever I needed help.

I would like to thank Dr. Pınar Mercan for her support and sharing her experience on vapor generation system with me.

I would like to thank Cengiz Şimşek for dealing electrical problems of the atomizer used in the study. I should also thank Hamit Çağlar regarding preparation of glasswares. I also want to thank Halil Memiş for his help on Argon and Hydrogen gas tanks.

Last but not the least, I would like to thank my beloved family and friends for their moral support and encouragement. I am grateful to my mother Demet Çetmeli, my sisters Müge Çetmeli and Merve Uysal. I am thankful to Ege Özgüven for his endless support. Without their understandings, patience and moral support, it would be very difficult for me to complete this study.

TABLE OF CONTENTS

ABSTRACT v

ÖZ vii

ACKNOWLEDGEMENTS x

TABLE OF CONTENTS xi

LIST OF TABLES xiv

LIST OF FIGURES xv

LIST OF ABBREVIATIONS xix

CHAPTERS

1. INTRODUCTION 1

1.1. Selenium 1

1.1.1. Occurrence and Production 2

1.1.2. Applications of Selenium 2

1.1.3. Role of Selenium in the Body 3

1.1.4. Determination of Selenium 4

1.2. Atomic Absorption Spectrometry 5

1.2.1. Historical Development of AAS 5

1.2.2. Principle of AAS 5

1.2.3. Flame AAS (FAAS) 6

1.2.4. Graphite Furnace AAS (GFAAS) 6

1.3. Vapor Generation AAS (VGAAS) 7

1.3.1. Hydride Generation Atomic Absorption Spectrometry (HGAAS) 7

1.3.2. Photochemical Vapor Generation (PVG) 9

1.3.2.1. Development of PVG 9
1.3.2.2. Principle of Photochemical Vapor Generation 11
1.3.2.3. Mechanism of Photochemical Vapor Generation 12
1.3.2.4. Determination of Selenium by PVG 15
1.4. Atomization of Volatile Species 18
1.4.1. Quartz Tube Atomizers (QTA) 19
1.4.1.1. Flame-in-Tube Atomizers (FIT) 19
1.4.1.2. Externally Heated Quartz Tube Atomizers (EHQTA) 19
1.4.2. Tungsten Coil Atomizers 20
1.5. Atom Trapping and in situ Preconcentration Techniques 21
1.5.1. Slotted Quartz Tube Atom Trap (SQT-AT) 22
1.5.2. Water-Cooled U-Tube Atom Trap 22
1.5.3. Quartz and Metal Atom Traps with Vapor Generation 23
1.5.4. Tungsten Coil Atom Trap 23
1.6. Aim of the Study 24
2. EXPERIMENTAL 25
2.1. Chemicals and Reagents 25
2.2. Instrumentation 26
2.3. Photochemical Vapor Generation W-Coil Atomization Technique 27
2.4. UV-Photochemical Reactor 28
2.5. Atomization Unit 30
2.6. Procedures 32
2.6.1. Coating the Surface of Tungsten Coil 32
2.6.2. Experimental Procedure 33

2.6.3. Analysis of Selenium Dietary Supplement 34
2.6.4. Interference Study 34
3. RESULTS AND DISCUSSION 35
3.1. Optimization of Trapping and Atomization Temperatures 36
3.2. Optimization of Argon Flow Rate 41
3.3. Optimization of Hydrogen Flow Rate 42
3.4. Optimization of Concentration of Acetic Acid 43
3.5. Optimization of Sample Flow Rate 45
3.6. Optimization of Trapping Volume 46
3.7. Optimization of Irradiation Time 47
3.8. Coating of Tungsten Coil 48
3.9. Type of Organic Acid 50
3.10. Analytical Figures of Merit 52
3.11. Determination of Se (IV) in Selenium Dietary Supplements by CF-PVG W-Coil Atomization AAS 55
3.12. Interference Study 56
3.12.1. Interference of Elements Amenable to PVG 56
3.12.2. Interference of Transition Metals 59
3.12.3. Interference of Earth-Based Elements 64
4. CONCLUSION 71
REFERENCES 73

LIST OF TABLES

TABLES

Table 1.1. Dominant products of photochemical vapor generation [24] 11
Table 1.2. PVG studies of selenium in literature 18
Table 2.1. Instrumental parameters of Varian AA140 26
Table 2.2. Temperature program used for coating procedure 33
Table 3.1. Optimized Parameters for UV-PVG TCAAS 52
Table 3.2. Analytical Figures of Merit for CF-PVG W-coil AAS Technique 54

LIST OF FIGURES

FIGURES

Figure 1.1. Experimental set-up of PVG for the determination of selenium [26] 10
Figure 1.2. Simplified experimental set up of PVG (Adapted from Ref 23) 12
Figure 2.1. Schematic representation set up for continuous flow photochemical vapor generation 27
Figure 2.2. Schematic diagram of gas liquid separator 28
Figure 2.3. Photograph of UV lamp-Photochemical Reactor used in the study 29
Figure 2.4. Spectral transmittance of FEP tubing [62] 30
Figure 2.5. A laboratory made tungsten-coil atomizer used in this thesis study 31
Figure 2.6. Schematic representation of W-coil atomizer and quartz T-tube used in this study 32
Figure 3.1. Voltage vs. temperature relationship measured by thermocouple [64] 37
Figure 3.2. Voltage vs. Temperature Relationship measured by thermocouple and pyrometer [65] 37
Figure 3.3. Effect of trapping and atomization temperature on the absorbance signal of 50 μg/L Se (IV) in 0.5 M acetic acid solution. Argon flow rate: 200 mL/min, hydrogen flow rate: 400 mL/min, trapping volume: 6.0 mL, trapping period: 45 s, sample solution flow rate: 6.0 mL/min, irradiation time: 2.5 min. 39
Figure 3.4. The absorbance signals obtained at atomization temperature of 1665 ºC with different trapping temperatures (a) 487 ºC; (b) 643 ºC; (c) 703 ºC. 40
Figure 3.5. The absorbance signals obtained at trapping temperature of 643 ºC with different atomization temperatures: (a) 1575 ºC; (b) 1665 ºC; (c) 1462 ºC. 40
Figure 3.6. Effect of argon flow rate on the absorbance signal of 50 μg/L Se (IV) in 0.5 M acetic acid solution. Trapping temperature: 643ºC, atomization temperature: 1665ºC, hydrogen flow rate: 400 mL/min, trapping volume: 6.0 mL, trapping period: 45 s, sample solution flow rate: 6.0 mL/min, irradiation time: 2.5 min. 42

Figure 3.7. Effect of hydrogen flow rate on the absorbance signal of 50 µg/L Se (IV) in 0.5 M acetic acid solution. Trapping temperature: 643 ºC, atomization temperature: 1665 ºC argon flow rate: 200 mL/min, trapping volume: 6.0 mL, trapping period: 45 s, sample solution flow rate: 6.0 mL, irradiation time: 2.5 min. 43
Figure 3.8. Effect of acetic acid concentration on the absorbance signal of 50 µg/L Se (IV). Trapping temperature: 643 ºC, atomization temperature: 1665 ºC argon flow rate: 200 mL/min, hydrogen flow rate: 400 mL/min, trapping volume: 6.0 mL, trapping period: 45 s, sample solution flow rate: 6.0 mL, irradiation time: 2.5 min. 44
Figure 3.9. Effect of sample flow rate on absorbance signal of 50 µg/L Se (IV) in 0.5 M acetic acid solution. Trapping temperature: 643 ºC, atomization temperature: 1665 ºC, argon flow rate: 200 mL/min, hydrogen flow rate: 400 mL/min, trapping volume: 6.0 mL, irradiation time: 2.5 min. 46
Figure 3.10. Effect of sample volume on absorbance signal of 50 µg/L Se (IV) in 0.5 M acetic acid solution. Trapping temperature: 643 ºC, atomization temperature: 1665 ºC argon flow rate: 200 mL/min, hydrogen flow rate: 400 mL/min, sample solution flow rate: 6.0 mL, irradiation time: 2.5 minutes. 47
Figure 3.11. Effect of irradiation time on absorbance signal of 50 µg/L Se (IV) in 0.5 M acetic acid solution. Trapping temperature: 643 ºC, atomization temperature: 1665 ºC argon flow rate: 200 mL/min, hydrogen flow rate: 400 mL/min, trapping volume: 6.0 mL, trapping period: 45 s, sample solution flow rate: 6.0 mL/min. 48
Figure 3.12 . Effect of coating element on absorbance signal of 50 µg/L Se (IV) in 0.5 M acetic acid solution. Trapping temperature: 643 ºC, atomization temperature: 1665 ºC argon flow rate: 200 mL/min, hydrogen flow rate: 400 mL/min, trapping volume: 6.0 mL, trapping period: 45 s, sample solution flow rate: 6.0 mL/min. 50
Figure 3.13. Calibration plot of Se (IV) in 0.5 M acetic acid solution. 53
Figure 3.14. Linear range of calibration plot for Se (IV) 53
Figure 3.15. Interference effect of antimony on absorbance signal of 50 µg/L Se (IV) in 0.5 M acetic acid. Trapping temperature: 643 ºC, atomization temperature: 1665 ºC argon flow rate: 200 mL/min, hydrogen flow rate: 400 mL/min, trapping volume: 6.0 mL, trapping period: 45 s, sample solution flow rate: 6.0 mL/min. 58

Figure 3.16. Interference effect of lead on absorbance signal of 50 µg/L Se (IV) in 0.5 M acetic acid. Trapping temperature: 643 ºC, atomization temperature: 1665 ºC argon flow rate: 200 mL/min, hydrogen flow rate: 400 mL/min, trapping volume: 6.0 mL, trapping period: 45 s, sample solution flow rate: 6.0 mL/min. 59
Figure 3.17. Interference effect of manganese on absorbance signal of 50 µg/L Se (IV) in 0.5 M acetic acid. Trapping temperature: 643 ºC, atomization temperature: 1665 ºC argon flow rate: 200 mL/min, hydrogen flow rate: 400 mL/min, trapping volume: 6.0 mL, trapping period: 45 s, sample solution flow rate: 6.0 mL/min. 60
Figure 3.18. Interference effect of nickel on absorbance signal of 50 µg/L Se (IV) in 0.5 M acetic acid. Trapping temperature: 643 ºC, atomization temperature: 1665 ºC argon flow rate: 200 mL/min, hydrogen flow rate: 400 mL/min, trapping volume: 6.0 mL, trapping period: 45 s, sample solution flow rate: 6.0 mL/min. 61
Figure 3.19. Interference effect of copper on absorbance signal of 50 µg/L Se (IV) in 0.5 M acetic acid. Trapping temperature: 643 ºC, atomization temperature: 1665 ºC argon flow rate: 200 mL/min, hydrogen flow rate: 400 mL/min, trapping volume: 6.0 mL, trapping period: 45 s, sample solution flow rate: 6.0 mL/min. 63
Figure 3.20. Interference effect of cobalt on absorbance signal of 50 µg/L Se (IV) in 0.5 M acetic acid. Trapping temperature: 643 ºC, atomization temperature: 1665 ºC argon flow rate: 200 mL/min, hydrogen flow rate: 400 mL/min, trapping volume: 6.0 mL, trapping period: 45 s, sample solution flow rate: 6.0 mL/min. 64
Figure 3.21. Interference effect of calcium on absorbance signal of 50 µg/L Se (IV) in 0.5 M acetic acid. Trapping temperature: 643 ºC, atomization temperature: 1665 ºC argon flow rate: 200 mL/min, hydrogen flow rate: 400 mL/min, trapping volume: 6.0 mL, trapping period: 45 s, sample solution flow rate: 6.0 mL/min. 66
Figure 3.22. Interference effect of aluminum on absorbance signal of 50 µg/L Se (IV) in 0.5 M acetic acid. Trapping temperature: 643 ºC, atomization temperature: 1665 ºC argon flow rate: 200 mL/min, hydrogen flow rate: 400 mL/min, trapping volume: 6.0 mL, trapping period: 45 s, sample solution flow rate: 6.0 mL/min. 67
Figure 3.23. Interference effect of silicon on absorbance signal of 50 µg/L Se (IV) in 0.5 M acetic acid. Trapping temperature: 643 ºC, atomization temperature: 1665 ºC

argon flow rate: 200 mL/min, hydrogen flow rate: 400 mL/min, trapping volume: 6.0 mL, trapping period: 45 s, sample solution flow rate: 6.0 mL/min. 68
Figure 3.24. Interference effect of sodium on absorbance signal of 50 µg/L Se (IV) in 0.5 M acetic acid. Trapping temperature: 643 ºC, atomization temperature: 1665 ºC argon flow rate: 200 mL/min, hydrogen flow rate: 400 mL/min, trapping volume: 6.0 mL, trapping period: 45 s, sample solution flow rate: 6.0 mL/min. 69

LIST OF ABBREVIATIONS

AAS	Atomic Absorption Spectrometry
AFS	Atomic Fluorescence Spectrometry
GC	Gas Chromatography
GLS	Gas-Liquid Separator
GFAAS	Graphite Furnace Atomic Absorption Spectrometry
HGAAS	Hydride Generation Atomic Absorption Spectrometry
HG-ETAAS	Hydride Generation Electrothermal Atomic Absorption Spectrometry
EHQTA	Externally Heated Quartz Tube Atomizer
FAAS	Flame Atomic Absorption Spectrometry
FEP	Fluorinated ethylene propylene
FIT	Flame in Tube
HG	Hydride Generation
ICP-MS	Inductively Coupled Plasma-Mass Spectrometry
LOD	Limit of Detection
LOL	Limit of Linearity
LOQ	Limit of Quantitation
PTFE	Polytetrafluoroetylene
PVG	Photochemical Vapor Generation
SQT-AT	Slotted Quartz Tube Atom Trap
UV-PVG	Ultra-Violet Photochemical Vapor Generation
VGAAS	Vapor Generation Atomic Absorption Spectrometry
QTA	Quartz Tube Atomizer

CHAPTER 1

INTRODUCTION

1.1. Selenium

Selenium is a nonmetal element with atomic number of 34 and atomic mass of 78.96. It is in Group 16 together with oxygen, sulfur, tellurium and polonium. It belongs to Period 4 in the Periodic Table. Electron configuration of selenium is $[Ar]3d^{10}4s^{2}4p^{4}$. Selenium shows both metallic and nonmetallic properties [1].

Selenium was discovered by Jons Jacob Berzelius in Sweden in 1817. The name of the element comes from the moon goddess Selene [2].

Selenium has six naturally occurring isotopes including ^{74}Se, ^{76}Se, ^{77}Se, ^{78}Se, ^{80}Se, and ^{82}Se. Among these isotopes, the most abundant isotopes are ^{80}Se (49.82%) and ^{78}Se (23.52%) [1].

Selenium exists in several allotropic forms including hexagonal (gray), amorphous and monoclinic (red). At room temperature, stable form of selenium is hexagonal (gray) [3].

The chemical properties of selenium are between those of sulfur and tellurium. Chemical properties of selenium compounds show similarities to corresponding sulfur and tellurium compounds [1].

Selenium has four different oxidation states; Se (IV), Se (VI), Se (0) and Se (-II). The chemical forms of Se (IV) and Se (VI) are SeO_3^{-2} and SeO_4^{-2} in aqueous phase; Se (0) occurs in solid phase or colloidal form while Se (-II) is present as selenide e.g. Cu_2Se, HgSe, Ag_2Se in minerals, organic and biochemical compounds [4].

Selenium forms both ionic and covalent compounds; for instance, it forms several oxides by reacting with oxygen like SeO_2 and SeO_3 [3]. It makes ionic compounds such as Na_2Se, FeSe and Al_3Se_2. Selenium also forms binary compounds by reacting with metals e.g. Na_2SeO_3. Halides are formed with fluorine, chlorine and bromine [1].

1.1.1. Occurrence and Production

Selenium is a rare element. Its rank among 88 naturally occurring elements in the earth's crust is 70 [1]. Selenium is present in the Earth's crust in concentration between 0.05 to 0.09 μg/g. It mostly occurs as in the form of selenides (Se^{-2}) and selenites (Se^{4+}) together with sulfide (S^{-2}) minerals. It is found at high concentrations (120 μg/g) in extrusive volcanic rocks and sedimentary rocks. Selenium concentration is between 0.06 to 0.12 μg/L in seawater. Depending on pH of the water, the concentration of selenium could vary [5].

Selenium is widely distributed in Earth's crust and does not present at concentration high enough for mining. For this reason, selenium is produced as byproducts mainly from anode slimes which are output of electrolytic refining of copper. In electrolytic refining, sulfate-based electrolyte which does not solve precious and base metals is used. Therefore, selenium agglomerate at the bottom of the electrolytic cell. The amount of selenium depends on the ore from which the copper concentrate is derived. Slimes have selenium concentrations between 10% to 40% [6].

In 2011, the estimated world production of selenium was roughly 2000 tons. Selenium dioxide (SeO_2), sodium selenite (Na_2SeO_3), sodium selenate (Na_2SeO_4) and selenium oxychloride ($SeOCl_2$) are commercially available compounds of selenium [5].

1.1.2. Applications of Selenium

Selenium is used in numerous processes in industry. For instance, it is used as a decolorizing agent for green tint to remove iron impurities in the glass manufacturing. Cadmium sulfoselenide (Cd_2SSe) are used as pigments in plastics, ceramics, paints

and glass. These pigments offer some advantages: they are resistant to chemical and ultraviolet exposure and they have a good heat stability [1,5,6].

In the rubber industry, selenium is used as a vulcanizing agent. Its electronic uses include rectifier and photoelectric applications [5,6].

Selenium is also used in the production of solar cells. Copper indium selenide ($CuInSe_2$) can be the main compound used for solar cells in the future although the production process is costly [7].

Sodium selenite (Na_2SeO_3), sodium selenate (Na_2SeO_4), selenomethionine ($C_5H_{11}NO_2Se$) and selenocysteine ($C_3H_7NO_2Se$) are used as dietary supplement. These products are typically available in tablet form, in concentration up to 200 μg for per tablet. It was stated that this dosage is safe and sufficient for an average weight adult although it is higher than the recommended daily intake for selenium [1]. World Health Organization (WHO) proposed that selenium intake of 40 μg/day and 30 μg/day meet the needs of adult men and women, respectively [8].

The gamma emitting isotope, ^{75}Se has been used as a scanning agent in diagnostic applications of medicine [3].

Selenium is also used in agricultural applications. For example, sodium selenite (Na_2SeO_3) and sodium selenate (Na_2SeO_4) are used as additives in animal feeds and potassium ammonium sulfoselenide is used as an insecticide in glasshouses and crops. Moreover, selenium deficiency in soil is improved by adding selenium compounds to fertilizers [1].

1.1.3. Role of Selenium in the Body

Selenium was identified as an essential nutrient since 1950s, it was found that selenium could replace vitamin E in liver in the regime of chicks and rats for avoiding muscular, vascular, and hepatic lesions. Since then, diseases originating from the deficiency of selenium have been studied. Two types of diseases have been related to selenium deficiency: Keshan disease (a juvenile cardiomyopathy) and Kaschin-Beck

disease (chondrodystrophy)[9]. Both diseases have been observed in rural areas in Russia and China. Keshan disease led to the deaths of many people in China, specifically children. After that, it was found that their daily consumption of selenium was low (below 11 μg/day) [7].

Selenium is a fundamental constituent of selenoproteins. In recent years, thirty selenoproteins have been recognized throughout twenty five mammalian genes. Selenoproteins play significant role in various biological functions including DNA synthesis, antioxidant defense, formation of thyroid hormones, fertility and reproduction [10].

The selenoenzyme glutathione peroxidases, together with vitamin E, play a role in the protection of cells from oxidative attack. The activity of this enzyme in red blood corpuscles is associated with the selenium concentration up to 100 μg/L [7].

Selenium could be also converted into many metabolites in the organism. For example, one of the metabolites, methylselenol (CH_4Se) used in cancer treatment [10].

Selenium could be toxic at high concentration even though it is an essential element. For this reason, in the blood, selenium concentration should be between 60 and 100 μg/L. A chronic high selenium intake higher than 5 mg per day causes to symptoms like diarrhea, hair loss, changes of fingernails and effects on central nervous system [7].

1.1.4. Determination of Selenium

The concentration (ng/g) of selenium in biological and environmental samples is very low to detect with current analytical techniques, so sensitive techniques are required to be developed for the detection of selenium in various samples. Various analytical techniques have been used for the determination of total selenium such as atomic absorption spectrometry (AAS), atomic emission spectrometry (AES), atomic fluorescence spectrometry (AFS), inductively coupled plasma-atomic emission spectroscopy (ICP-AES) and inductively coupled plasma-mass spectrometry (ICP-MS) [5,11].

1.2. Atomic Absorption Spectrometry

1.2.1. Historical Development of AAS

The discovery of optical spectroscopy based on Sir Isaac Newton's observation of sunlight. He observed that when the sunlight passes through a prism, light splits into its colors. In 1802, with the discovery of black lines in sun spectrum by Wollaston, interests on this subject has increased among scientists. Fraunhofer named the strongest black lines starting from red end of the spectrum. The name Sodium D line is still used today. These black lines were attributed to absorption processes which occurs at sun's atmosphere by Brewster in 1820.

Alan Walsh, who introduced AAS as an analytical technique in his paper in 1955, is known as the father of modern AAS. In 1962, Perkin Elmer Corp. produced the Model 303 AAS according to Walsh's ideas [12].

1.2.2. Principle of AAS

Atoms of elements absorb at wavelengths which are specific to each element. In AAS, line sources which emit light in the element-specific wavelengths are usually used. A beam of light coming from this light source is passed through the atomized sample in the atomizer. The degree of absorption is directly proportional to the number of atoms in the measurement zone [13].

A typical light source used in AAS instrument is hollow cathode lamp (HCL). Flame or graphite furnace can be used as an atomizer. Selection of the specific wavelength is achieved by a monochromator. The selected light is directed to the detector which is usually a photomultiplier tube [13].

1.2.3. Flame AAS (FAAS)

Flame AAS is a widely used technique for elemental analysis due to its convenience and relatively freeness from interferences [14]. In this technique, the liquid sample is converted to aerosol form using a nebulizer. Then, the aerosol passes through spray chamber which is connected to flame head. The flame should have sufficient energy both for vaporization and atomization of the sample [12].

The most widely used flame in AAS applications is air-acetylene flame. It is preferred since it is easy to operate and allows sufficient sensitivity for most of the elements. It provides a suitable environment and a temperature (~2300°C) for atomization over 30 elements [12,14,15]. For the elements that require higher temperature for atomization, nitrous oxide-acetylene flame whose temperature reaches to ~3000°C is usually used [15].

1.2.4. Graphite Furnace AAS (GFAAS)

An electrothermal graphite furnace is used in GFAAS as an atomizer. In this technique, the sample is injected into graphite furnace and then, it is heated step by step to dry, ash the organic matter, vaporize and atomize analyte species [16].

In 1959, L'vov introduced graphite furnace to be used as an atomizer in AAS [17]. L'vov furnace involved a graphite platform to which the sample was injected and then, it is put into the graphite tube. Both solid and liquid samples can be analyzed by this furnace. Later, Massmann's furnace was introduced in 1968. There was no sample electrode present in this model. The operating cycle of this design included three main steps. First one is the drying process to vaporize solvent. Second step is the ashing stage to remove the matrix components except for analyte atoms. Last step is the atomization stage to produce free atoms of the analyte. Nowadays, commercially available graphite furnace AAS has the same design as Massmann's furnace [17].

The detection limit obtained with a graphite furnace is much better compared to the detection limit attained with flame AAS. Another advantage of GFAAS is that not

only liquid samples but also slurries and solid samples can be analyzed. Moreover, the atomization capability of this atomizer is much more effective than that of the flame furnace. Samples with small quantities could be analyzed in GFAAS [16].

1.3. Vapor Generation AAS (VGAAS)

Vapor Generation AAS is a sample introduction technique that provides determination of concentration of elements by converting them into gas phase species. Vapor generation technique includes three steps: (1) generation of volatile analyte species, (2) carrying volatile analyte species to atomizer, (3) decomposition of volatile analyte and measurement of the atomic absorption response. This technique provides many advantages. For instance, analyte is separated from its matrix and better sensitivity is also achieved due to higher efficiency of sample introduction. In addition, larger sample volume could be used and thus, better detection limits can be obtained [18].

There are different types of vapor generation techniques such as hydride generation, cold vapor generation and photochemical vapor generation. Among them, hydride generation is the most commonly used technique since it can be applied to elements forming volatile hydrides [19]. Cold vapor generation technique is mostly used for the determination of mercury [18].

1.3.1. Hydride Generation Atomic Absorption Spectrometry (HGAAS)

Starting from 1970s, Hydride Generation (HG) has been used for the determination of trace elements in aqueous samples. In this technique, volatile and insoluble hydrides of elements are formed and then, transferred to atomizer. This provides a way to determine some of the elements that cause problems when analyzed by conventional methods e.g. Flame AAS. The elements especially Group 14-16 are important in case of hydride generation since limit of detections of these elements could be improved by several order of magnitude by using HGAAS. As, B, Ge, In, Pb, Sb, Se, Sn, Te and Tl are determined by HGAAS [20].

Chemical vapor generation (CVG) that is performed using tetrahydroborate (III) is a popular technique for the determination of many elements in atomic spectrometry [21].

A mechanism behind chemical vapor generation was firstly proposed by Robbins and Caruso in 1979. They suggested that a nascent hydrogen, which is formed during the acid hydrolysis of tetrahydroborate (III) is responsible for the hydride generation of the element to be determined. Following reactions occur:

$$BH_4^- + H^+ + 3H_2O \rightarrow B(OH)_3 + 8H$$

$$M^{(m+)} + (m+n)\,H \rightarrow MH_n + mH^+$$

where m depicts the oxidation state of the analyte and n is coordination number of the hydride [21].

Later, to explain the mechanism of CVG, D'ulivo and coworkers used GC-MS with deuterium labeled reagents. In this study, the formation mechanism of stannane (SnH_4), arsine (AsH_3), bismuthine (BiH_3), germane (GeH_4), stibine (SbH_3), and hydrogen selenide (H_2Se) were studied by directing the volatile species to GC-MS. The compounds was produced by derivatization with $NaBD_4$ (TDB) or $NaBH_4$ (THB in aqueous solutions of Sn(IV), As(III), Bi(III), Ge(IV), Sb(III) and Se(IV). It was reported that a direct hydrogen transfer from boron to analyte atom occurs and hydrides are formed.[21] The following general reaction mechanism was proposed:

$$MY_n + L_3BH \leftrightharpoons \text{Intermediate} \rightarrow Y_{n-1}MH \rightarrow Y_{n-x}MH_x \rightarrow MH_n$$

Where L is H^-, H_2O, OH^- or Cl^-; Y is H_2O, OH^- or Cl^-.

According to this reaction model, hydrogen transfer from boron to analyte takes place following a rearrangement reaction of the intermediate. This leads formation of an intermediate analyte hydride specie which contain one hydrogen atom replacing a ligand group. Then, another intermediate hydride is formed until all the ligands originally bound to the analyte atoms are replaced by hydrogen. Finally, volatile hydride is obtained [21].

1.3.2. Photochemical Vapor Generation (PVG)

1.3.2.1. Development of PVG

Photochemistry deals with chemical reactions which occur under the influence of visible and ultraviolet light. First law of photochemistry, also known as Grotthus-Draper law, states that in order to a photochemical reaction to occur, the light must be absorbed by any component of the system [22].

UV region is divided into three parts. The wavelength range of 315-400 nm is named as UV-A while the wavelength range of 280-315 nm is named as UV-B and the wavelength range of 100-280 nm is called as UV-C. Spectroscopic use of UV-C region is seldom since irradiation on this range proceed under vacuum or purged conditions because of strong molecular absorption by atmospheric components such as ozone formation from dissolved oxygen in the solution [23]. However, photochemical vapor generation technique is performed in UV-C region by using suitable design of the light source [24]. For the design of photoreactor, PFA (perfluoroalkoxy), FEP (fluorinated ethylene propylene) and quartz tubing are usually used. When quartz is designed as photoreactor, vacuum UV region (i.e. 185 nm) can be used.

In 2000, it was shown by Kikuchi and Sakamoto that SeO_4^{2-} was converted into SeH_2 photocatalytically in formic acid in the presence of TiO_2 for investigating reduction reactions of selenate ions in aqueous solution [25]. Afterwards, this phenomenon was adapted to the determination of selenium by photochemical vapor generation technique in 2003 by Sturgeon and coworkers [26,27]. Volatile selenium compounds were formed by UV irradiation (254 nm) in the presence of low molecular weight organic acids such as formic acid, acetic acid, propionic acid, and malonic acid in the study by Guo and coworkers [26,27]. The experimental setup used in their study is given in Figure 1.1. The volatile species formed with UV irradiation were transferred into quartz T-tube atomizer. By cryotrapping GC-MS analysis, volatile selenium species were identified as selenium hydride (SeH_2), selenium carbonyl (SeCO), dimethyl selenide

(C_2H_6Se) and diethyl selenide ($C_4H_{10}Se$) in the presence of formic acid, acetic acid, propionic acid and malonic acid, respectively [26,27].

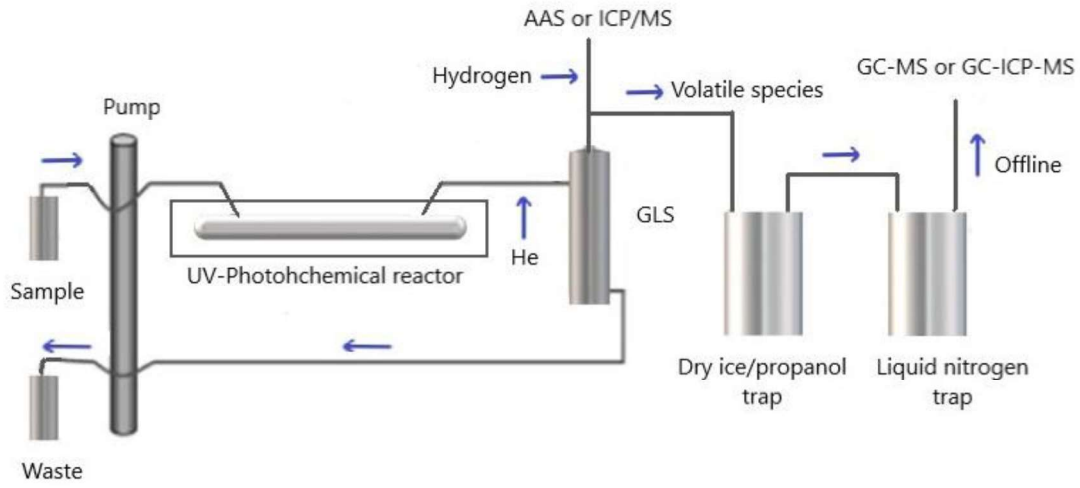

Figure 1.1. Experimental set-up of PVG for the determination of selenium [26]

Photochemical vapor generation has been implemented to elements which can be determined by CVG, such as As, Bi, Sb, Se, Sn, Te; to nonmetals Br and I and transition metals Cd, Co, Fe, Ni, Os [24]. Dominant products formed in PVG for these elements are given in Table 1.1. [24].

Table 1.1. *Dominant products of photochemical vapor generation* [24]

Analyte	Type of Carboxylic Acid			
	Formic Acid	**Acetic Acid**	**Propionic Acid**	**Reference**
Hg(II)	Hg^0	Hg^0	Hg^0	[28,29]
CH_3HgCI	Hg^0	Hg^0	Hg^0	[28,29]
Se(IV)	SeH_2/SeCO	$Se(CH_3)_2$	$Se(C_2H_5)_2$	[26,30]
Se(VI)	*NR** (TiO_2)	*NR*(TiO_2)	*NR* (TiO_2)	[26,30]
As(III/V)	AsH_3	$As(CH_3)_3$	$As(C_2H_5)_3$	[31,32]
I(-1)	HI	CH_3I	C_2H_5I	[33]
Br(-1)	HBr	CH_3Br	C_2H_5Br	[34]
Ni(II)	$NiCO_4$	$Ni(CO)_4$	-	[35]
Fe(II/III)	$Fe(CO)_5$	$Fe(CO)_5$	-	[36]
Co(II)	$Co(CO_4)H_2$		-	[37]

1.3.2.2. Principle of Photochemical Vapor Generation

Photochemical vapor generation is based on radical formation from aqueous solutions containing low molecular weight carboxylic acid by exposure to UV light source. A simplified set-up of a PVG process is given in Figure 1.2. Components of a photochemical vapor generation setup consist of a peristaltic pump, photoreactor, a gas liquid separator and an atomizer. The function of gas-liquid separator is to separate the volatile species from liquid phase. Argon or Helium gas is used to carry the volatile species to the detection part [24].

Photochemical vapor generation offers many advantages. For instance, use of $NaBH_4$, which is a potential source of contamination and unstable in aqueous solution, is eliminated in PVG technique. Moreover, the technique offers green chemistry to some extent since reagents and by-products are relatively environmentally friendly compared to CVG. PVG provides high efficiency for product generation, reduced interferences from concomitant elements and enhanced limit of detections. On the other hand, some interferences may arise from oxidants [24]. Since PVG works based

on reducing radical mechanism, possible interferences can be arisen from transition metals (Cu, Fe, Ni and Co) and common oxidants (dissolved oxygen, nitrate and nitrate ions) [24].

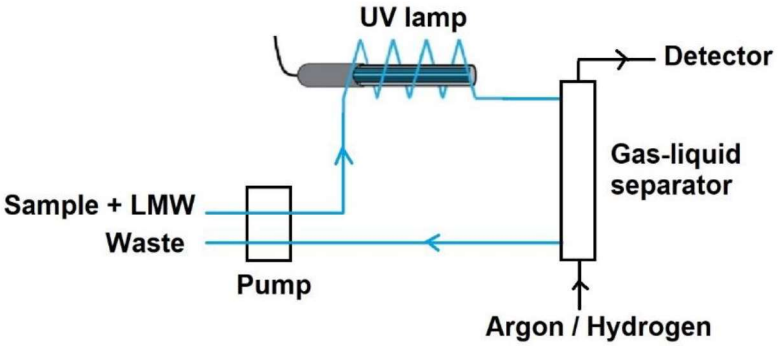

Figure 1.2. Simplified experimental set up of PVG (Adapted from Ref 23)

1.3.2.3. Mechanism of Photochemical Vapor Generation

The mechanism of photochemical vapor generation has not been comprehensively understood so far. However, according to the experimental data collected, an unanimity formed for the mechanism of PVG in the literature. According to this mechanism, PVG is an outcome of the radical reactions which are formed by the photolysis of carboxylic acids and ligand-to-metal charge transfer reductions and oxidations. PVG studies, which investigate the kind of volatile species and the effect of parameters on the PVG, support this mechanism [24].

For analytic applications of PVG, selenium was the first element studied. Although the catalyst TiO_2 was used to produce hydrogen selenide from the solutions of formic acid in the study of Kikuchi and Sakamoto, it was found later that the use of catalyst for PVG of Se (IV) is unnecessary [25–27]. Both hydrogen selenide (SeH_2) and selenium carbonyl (SeCO) were found to be formed in the presence of formic acid (HCOOH) while dimethyl-selenide (C_2H_6Se) was generated in the presence of acetic acid (CH_3COOH). It was also found that diethyl-selenide ($C_4H_{10}Se$) was produced in the presence of propionic acid (CH_3CH_2COOH).

Guo and coworkers suggested that photolytic cleavage of the low molecular organic acids yield hydrogen, carboxylate, methyl and carbonyl radicals and then these radicals reduce metal ions to produce alkylated, hydrogenated or carbonylated products of the element. For example, in a specific case where selenite was reduced in acetic acid solution, the following mechanism was suggested (unbalanced stoichiometry) [27,38]:

$$R\text{-}COOH + h\nu \rightarrow [RCOOH]^{*} \rightarrow {}^{\bullet}R + {}^{\bullet}COOH \rightarrow RH + CO_2$$

$$R\text{-}COOH + Se^{4+} \rightarrow CO_2 + R_2Se + 2RH + H_2$$

It was reported that H_2, CO, CH_4, CO_2 CH_3OH and C_2H_6, etc., may be stable end products of the photolysis of acetic and formic acids however, intermediate species may include reactive radicals such as H, CH_3, R and COOH (and likely radical anions, COO^-). Based on computational study, Takatani and coworkers suggested an alternative route: direct sequential attack of carbon monoxide or ketene on selenite through a series of reactions, taking into account the formation of selenium hydride and dimethylselenide [39]:

$$HCOOH + h\nu \rightarrow [HCOOH]^{*} \rightarrow H_2O + CO$$

$$CH_3COOH + h\nu \rightarrow [CH_3COOH]^{*} \rightarrow H_2O + CH_2CO$$

CO (carbonyl), formed as a result of the product of UV irradiation of formic acid, leads to following reaction mechanism for the production of selenium carbonyl (SeCO) proposed by Takatani and coworkers:

$$SeO_3^{2-} + CO \rightarrow SeO_2^{2-} + CO_2$$

$$SeO_2^{2-} + CO \rightarrow SeO^{2-} + CO_2$$

$$SeO^{2-} + CO \rightarrow Se^{2-} + CO_2$$

$$CO_2 + H_3O^{+} \rightarrow COOHOH_2^{+}$$

$$Se^{2-} + COOHOH_2^{+} \rightarrow SeCOOH^{-} + H_2O$$

$SeCOOH^- + H_3O^+ \rightarrow SeCO + 2H_2O$

However, Sturgeon and coworkers argued that this mechanism is unlikely since the transient intermediate ketene is not detected as a product of photolysis of any LMW carboxylic acids used in PVG. This species is unlikely to survive long enough in an aqueous solution to participate in a series of sequential chemical reactions with the selenite reduction intermediates [38].

Two different scenarios were proposed by Sturgeon and Grinberg to elucidate the mechanism of PVG of Se (IV) [24]. First scenario involves a redox sequence comprising the release of a hydrated electron by photolysis of HCO_2.

$HCO_2^- + h\nu \rightarrow HCO_2^\bullet + e_{(aq)}^-$

$HO\text{-}SeO\text{-}OH + e_{(aq)}^- \rightarrow HO\text{-}Se{=}O + HO^-$

$HO\text{-}Se{=}O + e_{(aq)}^- \rightarrow Se{=}O + HO^-$

$Se{=}O + e_{(aq)}^- \rightarrow Se^0 + O^-$

$Se^0 + O^- + H^+ \rightarrow Se^0 + OH$

$Se^0 + {}^\bullet R \rightarrow R\text{-}Se$

$Se\text{-}R + {}^\bullet R \rightarrow$ various products

The other scenario is related to cascade sequence of nucleophilic attacks by ●R and rearrangements as shown in the following reaction scheme [24]:

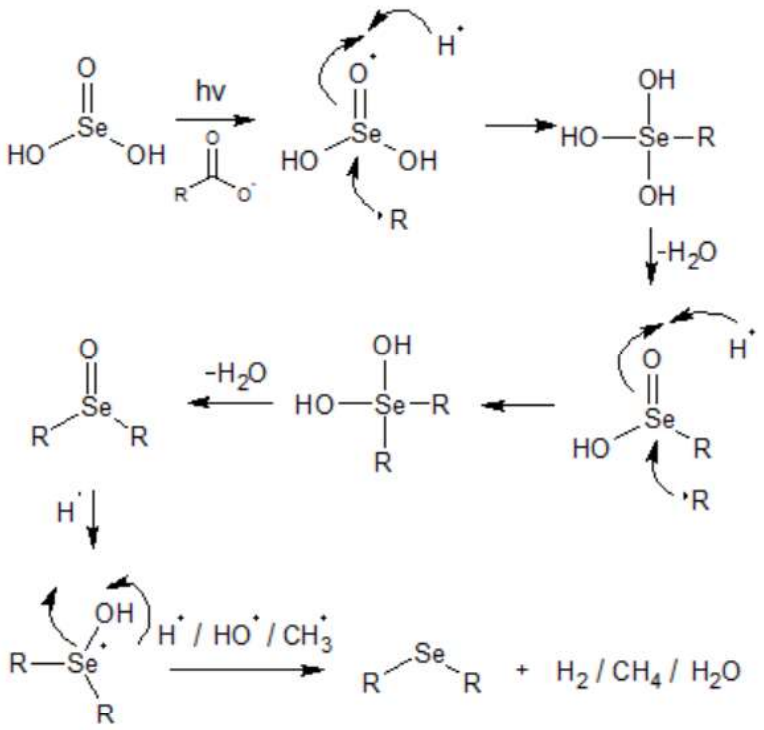

1.3.2.4. Determination of Selenium by PVG

For analytical purpose of photochemical vapor generation, selenium was the first element studied [26,27]. Volatile selenium compounds were formed by UV irradiation in the presence of low molecular weight organic acids by Guo and coworkers. The experimental setup is given in Figure 1.1. The volatile species produced with UV irradiation were directed to quartz T-tube atomizer for the detection of selenium atoms by atomic absorption spectrometer.

In 2008, Zheng and coworkers coupled PVG to AFS or ICP-MS, based on Se (IV) or Se (VI) reacting with an organic acid (formic acid/ acetic acid/ propionic acid) [40]. It has been found that, when boiling water bath and nano-TiO_2 (as a catalyst) was used, both Se (IV) and Se (VI) can be photochemically converted to selenium volatile species, thus total Se was determined [40].

In an another study by Yang and coworkers, nano-TiO_2 was used as both catalyst and adsorbent [41]. Yang and coworkers developed a method to determine total selenium concentration in water samples by using AFS. Se (IV) and Se (VI) were adsorbed on slurry of TiO_2 nanoparticles. Then, in formic acid solution, these nanoparticles were exposed to ultraviolet light to obtain volatile selenium species. It was reported that sensitivity improvement by 56-fold was obtained with this preconcentration step.

In 2015, UV-photochemical vapor generation in combination with in situ collection of volatile compounds in the graphite tube atomizer AAS was employed for the determination selenium (IV). Iridium was used as a modifier [42]. Selenium (IV) in formic acid (HCOOH) solutions were exposed to UV irradiation. They also studied the effect of addition of nitric acid (HNO_3) to the Se (IV) solutions. When both formic acid (HCOOH) and nitric acid (HNO_3) were present in the solution, selenium signal enhanced or depressed depending on nitric acid concentration. Addition of sodium nitrate to the solution also resulted in improvement of the signal. It was deduced that nitrate anion is responsible for the signal improvement.

Rybínová and coworkers used quartz furnace-AAS as atomizer when UV photochemical vapor generation was employed for the determination of the selenium in five selenium dietary supplements [43]. The form of the selenium in these tablets were sodium selenite (Na_2SeO_3) or sodium selenate (Na_2SeO_4). For tablets containing Se (VI), prereduction to Se (IV) step was included in sample preparation. For this reason, the solution containing Se (VI) was heated to 90 ºC for sixty minutes in 6 M HCI. As a photochemical agent, formic acid and acetic acid were used. In the presence of formic acid, better sensitivity was obtained even with shorter reaction coil compared to acetic acid [43].

In 2016, Rybínová and coworkers investigated the effect of several modifications of UV-photochemical reactor on PVG of selenium. Externally heated quartz furnace atomizer was used to detect volatile species. They have studied the type of material used for reaction coil tubing and dimensions of the tubing. When sensitivities, LODs

and repeatability were compared, it was found that teflon is a good competitor for quartz tubing. Since the construction of photochemical reactor with teflon is easier and cheaper than quartz, teflon tubing can be used unless irradiation at 185 nm is required [44].

In another study, PVG of selenium was studied using flow-injection AFS. A germicidal mercury-based lamp that emits at 185 and 254 nm was used in UV-photochemical reactor. FEP (fluorinated ethylene propylene) tubing was used to construct the photoreactor. Formic acid concentration was between 0.3 and 0.5%[30]. The generated volatile specie with photo-CVG of Se (IV) in the presence of formic acid was detected as selenium carbonyl (SeCO) by GC-MS analysis [30].

All of the studies with PVG to determine selenium summarized in this section are given in Table 1.2.

Table 1.2. *PVG studies of selenium in literature*

Se species	Atomizer	Organic acid	LOD	Type of UV lamp and its wavelength	Reference
Se(IV)	Quartz tube atomizer	Formic acid, Acetic acid, Propionic acid and Malonic acid	0.0025 mg/L (acetic acid)	Low-pressure Hg vapor UV lamp (254 nm)	26,27
Se(IV) and Se(VI)	Argon-hydrogen flame in quartz atomizer	Formic acid, Acetic acid, Propionic acid, Mixture of formic acid and 10 mmol HNO_3	0.1 µg/L (Se(IV) and Se(VI) in acetic acid) 0.1 µg/L (Se(V) and Se(VI) in formic acid) 0.08 µg/L Se(IV) and 0.05 µg/L (Se(VI) propionic acid)	High-pressure Hg vapor UV lamp	40
Se(IV) and Se(VI)	Argon-hydrogen flame	Formic acid	0.0008 µg/L (Se(IV) and Se(VI) with preconcentration	Low pressure UV lamp (254 nm)	41
Se(IV)	Graphite tube atomizer	Formic acid	4.1 ng/L	A low-pressure mercury UV bench lamp (254 nm)	42
Se(IV) and Se(VI)	Quartz furnace	Formic acid/ Acetic acid	40 ng/L (formic acid)	A low-pressure mercury UV bench lamp (254 nm)	43
Se(IV)	Externally heated quartz furnace atomizer	Formic acid/ Acetic acid	33 ng/L (Quartz tubing, formic acid) 27 ng/L (Teflon tubing, formic acid)	A low- pressure mercury UV bench lamp (254 nm)	44
Se(IV)	MDF (miniature diffusion flame) atomizer	Formic acid/ Acetic acid	0.10 µg/L (acetic acid)	Germicidal low power ultraviolet mercury-based lamp (185 and 254 nm)	30

1.4. Atomization of Volatile Species

There are different types of atomizers used in AAS such as flame, plasma, quartz-T tube, graphite furnace. An ideal atomizer should fulfil the following requirements: First, analyte species should be completely converted into free atoms; second long residence time of atoms in the atomizer is required to obtain high sensitivities, third, signal to noise ratio should be high for better detection limits. User friendliness and low running cost are other requirements of an ideal atomizer [45].

Some of the atomization techniques coupled with vapor generation are summarized in the following sections:

1.4.1. Quartz Tube Atomizers (QTA)

Quartz tube atomizers (QTA) are usually quartz T-tubes with the horizontal arm that is aligned in the optical path of AAS instrument. Volatile compounds carried with a carrier gas are introduced from central arm of the T-tube. T-tube design is the most popular QTA, but L-tube design of QTA is also used [45].

Quartz T-tube atomizers are divided into two groups: externally heated quartz tube atomizers (EHQTA) and flame-in-tube atomizers (FIT).

1.4.1.1. Flame-in-Tube Atomizers (FIT)

A flame-in-tube atomizer was first used by Siemer and Hageman [45]. In a flame-in-tube atomizer, a capillary tube is positioned on the arm of the T-tube to provide a flow of oxygen in order to obtain a hydrogen–oxygen diffusion microflame. To form a microflame inside the tube, the carrier gas is mixed with hydrogen gas as a fuel. The temperature of the microflame is controlled by flow rate of oxygen gas. Hydrogen radicals are formed in the microflame as a result of the formation of the flame with a temperature of around 2800 °C [45].

1.4.1.2. Externally Heated Quartz Tube Atomizers (EHQTA)

Externally heated quartz tube atomizers are heated either by an electrical resistance device or acetylene-air flame. A temperature range of 700-1000 °C is obtained. A small portion of hydrogen with the carrier gas argon should be used for atomization. Usually, hydrogen is present in the medium because of the decomposition of tetrahydroborate. A special tube is not needed for the introduction of oxygen to atomizer in EHQTA. However, an oxygen content is necessary in the gas mixture for optimum sensitivity. Oxygen provides the formation of hydrogen radical cloud which is necessary for efficient atomization. Similar to FIT atomizers, H radicals are formed in the atomizer as a result of the reaction between hydrogen and oxygen at high temperature [45]. Following reactions have been proposed by Dedina and Rubeska [46]:

$H + O_2 \rightarrow OH + O$

$O + H_2 \rightarrow OH + H$

$OH + H_2 \rightarrow H_2O + H$

Oxygen demand depends on several factors: atomization temperature, diameters of the atomizer and total gas flow rate to atomizer [47]. Under typical atomization conditions, this demand is usually provided by contaminant oxygen (reagent solutions and gases). The analyte atoms in this medium are stable if there are enough H radicals. When there are no sufficient hydrogen radicals, analytes are in the form of molecular species. With excess hydrogen radicals, this can be overcome [45]. For instance, in case of SeH_2, following reactions take place in the presence of H radicals:

$SeH_2 + H \rightarrow SeH + H_2$

$SeH + H \rightarrow Se + H_2$

1.4.2. Tungsten Coil Atomizers

The specifications of an optimal electrothermal atomizer enclose high purity, high melting point, fast heating rate, physical and chemical stability, durability and inertness [48]. High purity graphite atomizers are excellent example of optimal atomizers; thus, they are common in commercial AAS instruments. With the need for a cost-efficient, portable and compact instrumentation, a tungsten coil atomizer has begun to be used instead of graphite furnaces. Among all the metals in the periodic table, tungsten has the highest melting point (3422 °C) [49]. Tungsten atomizers are desirable since they are relatively chemically inert and economical. To obtain fast heating rates and temperatures, lower power is needed with tungsten coils atomizers. Moreover, the tungsten coils cool very rapidly [50].

The use of tungsten as an atomizer dates back to early 1970s. Tungsten filament from a commercial light bulb as an atomizer was used in atomic absorption spectrometry for the first time in 1972. A double layer tungsten coil filament, which was produced

for 150 W lamps, was introduced in 1988 by Berndt and Schaldach to be used as an electrothermal atomizer. Since that time, 150 W tungsten coil has started to be used as an electrothermal atomizer [50].

Hou and coworkers reported that tungsten coil coated with iridium could be used for the determination of selenium in water samples. Iridium coating provided a longer lifetime of the coil (approximately 1600 firings) and using higher pyrolysis temperature. LOD of iridium coated tungsten coil was found to be 10 times better than that for FAAS. On the other hand, it is ten times higher than those obtained by conventional GFAAS [51].

1.5. Atom Trapping and in situ Preconcentration Techniques

Sample nebulization is a conventional method for sample introduction to the flame atomizer. However, this sample introduction method suffers from poor sample transport efficiency. The efficiency of sample transport with nebulizer to burner is between 1 and 10% depending on type of the nebulizer. As a result, very little amount of the analyte transports to the atomizer and sample dilution occurs because of flame gases. Moreover, residence time of the analyte is short in the flame. Sensitivity of FAAS is negatively influenced by both these drawbacks. Thus, several techniques have been suggested to enhance the sensitivity of FAAS [52].

To enhance the sensitivity of FAAS, different techniques have been suggested. Electrothermal atomization and hydride generation ensured an improvement in the sensitivity in the order of 100-1000 times compared to FAAS. However, since FAAS is more practical than other atomization techniques, several methods have been suggested to increase the sensitivity of FAAS. The main goal is to obtain longer residence time in the measurement zone. One of the widely studied approach is to trap the analyte on a surface to increase the number of atoms in the measurement zone. Trap means simply a delay for atomic species in the measurement zone. afterwards, revolatilization and atomization take place [52].

There are several approaches to trap the analyte given in the following sections:

1.5.1. Slotted Quartz Tube Atom Trap (SQT-AT)

The slotted quartz tube atom trap was introduced by Watling in 1977 to determine trace metals in fresh water samples [53]. In this study, a quartz tube containing upper and lower slots was positioned on top of the burner head. By using air-acetylene flame, up to ten fold increase in sensitivity was obtained depending on the type of the element [53]. Later, another study with SQT were published by Watling. In this study, signals of As Sb, Se and Hg elements in a multielement standard solution were measured and a threefold increase in absorbance signal was observed when the SQT was used compared to conventional FAAS [54]. In the other study by Watling, Pb, Zn, Cd, Bi, Co, Mn and Ag elements in composite multi-element standards were determined. A significant improvement in precision at low concentrations was obtained when the slotted tube was used compared to FAAS [55]. Thorburn and coworkers coupled SQT with hydride generation AAS to determine tin [56] and bismuth [57] in a copper-based alloys.

Later, SQT appeared to be used as an atom trap. This process involves three steps: collection, revolatilization and atomization. In the collection period, analyte species are trapped on the surface of the slotted quartz tube. This step lasts few minutes and then, an organic solvent is introduced into flame and a change in the composition of the flame is observed. This change is not related to temperature; in fact, flame conditions became more reducing with organic solvent aspiration. Thus, collected analyte species are released in the revolatilization step. This step followed by atomization and a transient signal is obtained [52].

1.5.2. Water-Cooled U-Tube Atom Trap

Use of water-cooled U-Tube atom trap was first shown in 1976 [58]. The tube which was made of silica, was placed in the laminar flame. Through U-tube, tap water is circulated so that the analyte species can be condensed on the cold surface of the silica tube. After the collection period, water flow around the tube is stopped and this results in increase in the temperature of the tube and thus, revolatilization and atomization of

the collected analyte species takes place. Finally, a transient signal of analyte is observed. Another trap system, a water cooled U-shaped silica trap coupled with slotted silica tube, was introduced by Ertaş and coworkers to combine advantages of both systems [59].

1.5.3. Quartz and Metal Atom Traps with Vapor Generation

In this atom trapping technique, HGAAS set-up is used. Karadeniz and coworkers was used HGAAS coupled to atom trapping to determine lead [60]. To obtain a trap zone, some crushed quartz particles were placed into the quartz tube atomizer (QTA). This part of the tube was heated externally by using a resistively heated wire. The analyte in HCI solution reacted with sodium tetrahydroborate (III) to produce volatile lead hydride, PbH_4. Gaseous lead hydride was separated from the liquid phase using a gas-liquid separator (GLS). The resultant vapor was transferred to the QTA where the PbH_4 was trapped. Then, revolatilization took place by increasing the temperature of the trap surface. Finally, a transient signal was measured. Quartz trap has been applied for the determination of other elements such as Sb, Bi, As, Cd and Se [52].

1.5.4. Tungsten Coil Atom Trap

In tungsten coil atom traps, tungsten coil is heated resistively. Higher heating rates is used compared to quartz trap since external heating is used in quartz traps. The tungsten coils are obtained from commercially available lamps therefore, they are very economical.

Tungsten coil atomizer was used for trapping which was reported by two groups in 2002 [50,61]. Barbosa and coworkers used tungsten coil atomizer for both trapping selenium hydride on the surface of tungsten and for atomization process. Selenium hydride trapped onto a double-layer coiled tungsten filament coated with rhodium [50]. Cankur and coworkers trapped bismuthine formed by reducing with sodium tetrahydroborate on heated tungsten coil [61]. It was reported that LOD values was comparable with or better than those achieved by HG-ETAAS and ICP-MS.

1.6. Aim of the Study

Photochemical vapor generation (PVG) is a relatively new method in atomic spectrometry. It offers many advantages: green chemistry, enhanced limit of detections, high efficiency for the volatile specie generation, reduced interferences from concomitant elements, elimination of the use of fresh chemical reductant, simplified laboratory device requirements [24].

PVG was used for the determination of selenium [26,27,30,40–43]. In these studies, selenium was determined using various atomization techniques such as graphite/quartz furnace, quartz/graphite tube atomizer. In this study, volatile species generated from PVG of selenium was both trapped and atomized using tungsten coil atomizer. Thus, both the advantages of PVG and the advantages of the tungsten coil atomizer are combined in this study.

CHAPTER 2

EXPERIMENTAL

2.1. Chemicals and Reagents

All reagents used throughout this study were of analytical grade or higher purity. Working solutions of Se (IV) were prepared daily by successive dilutions of 1000 mg/L Se (IV) stock solution in water (High Purity Standards). Dilutions were done using 18.2 MΩ cm deionized water from Elga Purelab Option-Q Water Purification System.

High purity Argon (99.999 %, Linde) and Hydrogen (99.999 %, Linde) gases were used throughout the study.

Acetic acid (Sigma Aldrich), formic acid (Merck) and propionic acid (Acros Organics) were used as low molecular weight organic acids. All glasswares and plastics were immersed in 10% (v/v) HNO_3 for at least 24 hours and washed with distilled water and then, rinsed with deionized water.

For coating process, 1,000 mg/L Rh solution in 10% HCI (Source: $RhCI_3$,(rhodium (III) chloride) High Purity Standards), 1,000 mg/L Ir in 2% HCI (Source: $IrCI_3.3H_2O$, (iridium (III) chloride trihydrate) High Purity Standards), 1,000 mg/L Pd in 10% HNO_3 (Source: Pd (palladium) High Purity Standards) and 1,000 mg/L Co in 2% HNO_3 (High Purity Standards) solutions were used. 1,000 mg/L Ru solution was prepared from ruthenium chloride hydrate ($RuCI_3.H_2O$) by dissolving the appropriate amount in %20 (v/v) HCI solution.

For interference study, following chemicals were used. To obtain 1,000 mg/L Sb, appropriate mass of potassium antimony tartrate ($C_4H_4KO_7Sb$) (Sigma-Aldrich) was

weighed ant dissolved in deionized water. 1,000 mg/L Pb stock solution in HNO_3 (Fisher Scientific), 1,000 mg/L Mn stock solution in HNO_3 (Fisher Scientific), 1,000 mg/L Ni stock solution in HNO_3 (Fisher Scientific), 1,000 mg/L Si stock solution (source: ammonium hexafluorosilicate ($(NH_4)_2SiF_6$), Fisher Scientific), 1,000 mg/L Cu stock solution in 0.5 mol/L HNO_3 (source: $Cu(NO_3)_2$ (copper(II) nitrate) Merck), 1,000 mg/L Ca stock solution in 0.5 mol/L HNO_3 (source: $Ca(NO_3)_2$ (calcium nitrate), Merck), 1,000 mg/L Al stock solution in 0.5 mol/L HNO_3 (source: $Al(NO_3)_3$, (aluminum nitrate), Merck), were used for the interference study of lead (Pb), manganese (Mn), nickel (Ni), silicon (Si), copper (Cu), calcium (Ca) and aluminum (Al) respectively. Necessary dilutions were made using deionized water.

2.2. Instrumentation

Varian AA140 Atomic Absorption Spectrometer (Victoria, Australia) was used throughout this study. The instrument is equipped with deuterium background correction system. SpectrAA software was used to process the data. The instrumental parameters are given in the Table 2.1. Selenium Hollow cathode lamp (Photron, Australia) was used.

Table 2.1. *Instrumental parameters of Varian AA140*

Parameter	**Value**
Wavelength, nm	196
Lamp current, mA	10
Measurement mode	Peak Height

2.3. Photochemical Vapor Generation W-Coil Atomization Technique

The analyses were performed in continuous flow mode using peristaltic pumps (Minipuls 3, Gilson). Polytetrafluoroethylene (PTFE, Cole Parmer) tubing with I.D.:0.81 mm and O.D.:1.42 mm connected to yellow/blue coded 2-Stop Tygon® tubing (I.D: 1.52 mm) was used for carrying sample or blank solutions to photochemical reactor. Schematic diagram of continuous flow photochemical vapor generation system is given in Figure 2.1.

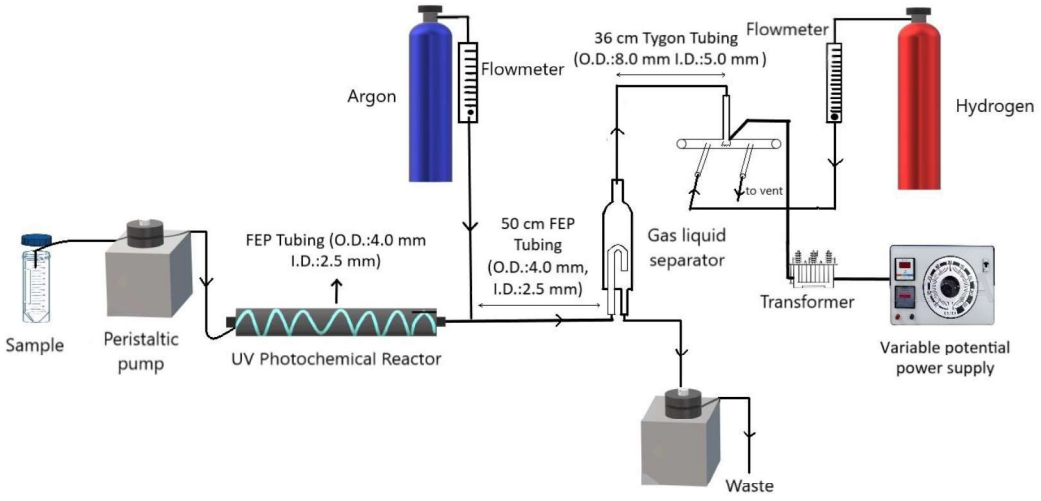

Figure 2.1. Schematic representation set up for continuous flow photochemical vapor generation

UV photochemical reactor is placed after the peristaltic pump. UV-photochemical reactor is designed by wrapping the UV lamp (LightTech, 254 nm, 40 watt, 43.6 cm) with fluorinated ethylene propylene (FEP) tubing with 4 mm of O.D. and 2.5 mm of I.D. (Parker). Totally 50 m FEP tubing was used to coil the reactor.

Ar gas was used as a carrier gas. Hydrogen gas is introduced directly to the Quartz T tube in order to prevent oxidation of tungsten coil inside the Quartz tube and to increase the atomization efficiency of selenium from the surface of the coil.

Rotameters (Cole-Parmer) were used to control the flow rates of the gases. Both rotameters were calibrated using a laboratory made soap bubble meter.

A cylindrical type gas liquid separator (GLS) was used to separate volatile species from liquid phase. It was made by Glass Blower at Department of Chemistry, METU. A schematic representation of GLS is given in Figure 2.2. Another peristaltic pump Ismatec, Cole-Parmer) was used to carry the liquid phase from gas liquid separator. Top of the GLS is connected to the W-coil atomizer with a 36 cm long Tygon tubing (O.D.:8.0 mm, I.D.:5.0 mm).

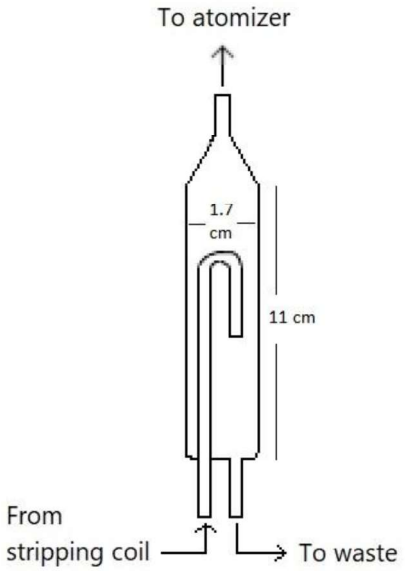

Figure 2.2. Schematic diagram of gas liquid separator

2.4. UV-Photochemical Reactor

UV-photochemical reactor was prepared by coiling the UV-lamp with fluorinated ethylene propylene (FEP) tubing with 4 mm of O.D. and 2.5 mm of I.D. (Parker). FEP tubing was selected since it transmits a high percentage of ultraviolet light. Spectral transmittance of FEP polymer is given in Figure 2.4. The temperature of the sample solution inside FEP tubing increases due the increase in the temperature of the UV

lamp. Therefore, to keep the temperature (45°C) of the solution passing through the FEP tubing another layer of tubing which carries the cold water at 4 °C was coiled on the surface of the FEP tubing carrying the sample solution. Peristaltic pump (Longerpump) was used to pump continuously the cold water. While the lamp was on, the lamp is wrapped by a cardboard to block the UV light reaching to the laboratory working medium. The UV-photochemical reactor used in the study is given in Figure 2.3.

Figure 2.3. Photograph of UV lamp-Photochemical Reactor used in the study

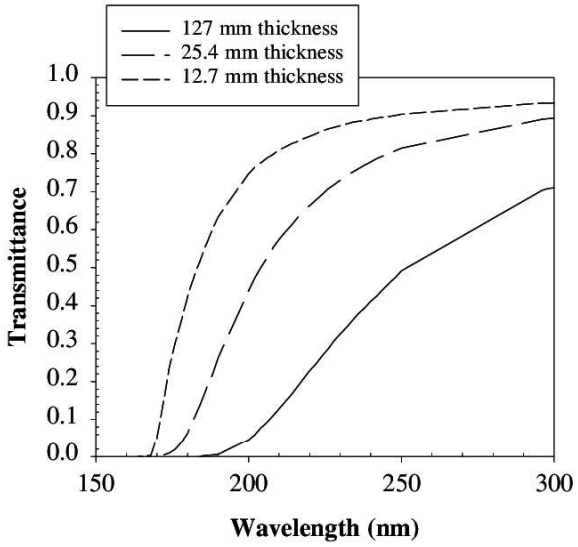

Figure 2.4. Spectral transmittance of FEP tubing [62]

2.5. Atomization Unit

W-coils were obtained from a 15 V, 150 W projection lamp Type 6550 (Philips, Germany) used as both atomizer and trapping medium in this study. Photograph of W-coil atomizer used in this study is shown in Figure 2.5.

Figure 2.5. A laboratory made tungsten-coil atomizer used in this thesis study

The temperature of the coil was controlled by a power supply (Variac, Şimşek Laborteknik, Turkey). A 750 W transformer was placed between Variac and the coil to decrease the voltage. A multimeter (LG, DM-341) was used to measure the applied voltage to W-coil. W-coil was placed into a glass apparatus which was built by Glass Shop in the Department of Chemistry, METU. Quartz windows were glued to the each side of the T-tube in order to prevent oxygen diffusion since oxygen oxidize tungsten coil. Hydrogen gas is directed into one of the tube attached to the Quartz T-tube and from the other tube H_2, Ar and all gases produced from the surface of the coil are directed to the vent of the laboratory. W-coil atomizer is represented in Figure 2.6. It is put on top of the burner head of AAS.

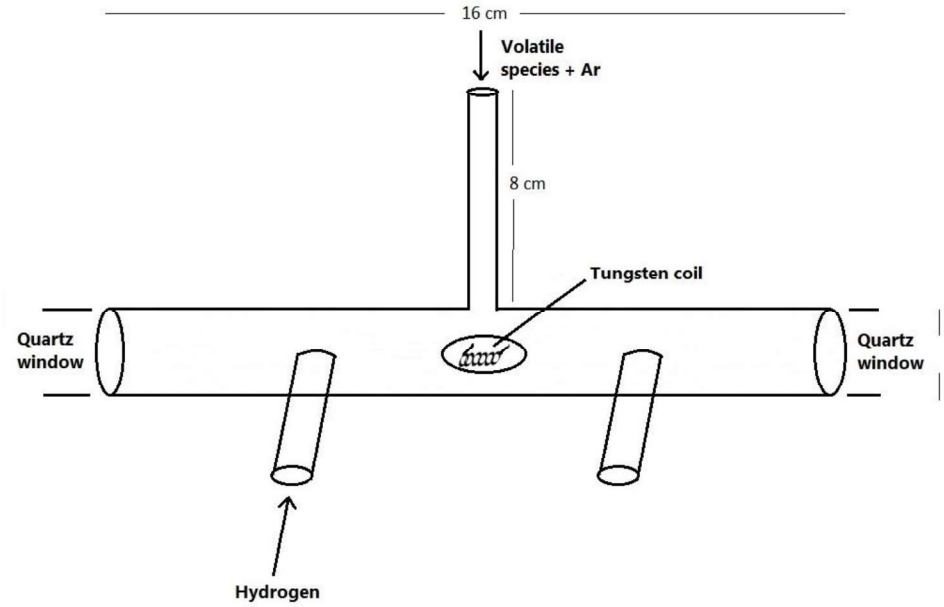

Figure 2.6. Schematic representation of W-coil atomizer and quartz T-tube used in this study

2.6. Procedures

2.6.1. Coating the Surface of Tungsten Coil

The surface of tungsten coil was coated with different elements. While choosing the coating elements, elements having high boiling points were selected in order not to lose the material from the surface of the coil. Rh, Ru, Ir, Co and Pd coatings were used in this study.

For coating procedure, 20 µL of 1000 mg/L stock solution of Rh, Ru, Ir, Co or Pd was pipetted onto the surface of W-coil. For each coating, an unused W-coil was used. The temperature program given in Table 2.2 was applied sequentially after injecting the coating solution. Ten times this procedure was repeated in order to make sure that the surface of the coil was coated homogenously with the coating element. Totally, 2 mg of coating element was coated on the surface of tungsten coil.

Table 2.2. *Temperature program used for coating procedure*

Temperature (ºC)	Time (s)
50	60
487	30
679	10
1318	3

2.6.2. Experimental Procedure

The solutions containing Se (IV) and 0.5 M of acetic acid were passed through the system via peristaltic pumps with a 6.0 mL/min flow rate. The solution was passed through the UV-photochemical reactor. After the solution reached to end of reactor, argon flow of 200 mL/min was introduced into the system in order to carry the volatile species to the gas-liquid separator. Afterwards, volatile species were carried to W-coil atomizer with Ar flow. Hydrogen gas with flow rate of 400 mL/min was directed to the atomizer. Volatile species of selenium were trapped on the surface of W-coil for 45 seconds. At trapping step, tungsten coil temperature was kept at 643ºC. After collection period, peristaltic pumps were stopped and then, atomization took place by heating tungsten coil to 1665ºC. Finally, a transient signal was obtained for selenium.

The following experimental parameters were optimized sequentially:

- Trapping temperature
- Atomization temperature
- Flow rate of argon gas
- Flow rate of hydrogen gas
- Concentration of the acetic acid
- Trapping volume
- Trapping period

- Irradiation time
- Type of the acid

2.6.3. Analysis of Selenium Dietary Supplement

CF-PVG method was applied to selenium dietary supplements (Meka Nutrition) to determine selenium concentration in the tablets. The tablets are composed of the following ingredients: sodium selenite (Na_2SeO_3), microcrystalline cellulose and lactose monohydrate.

Following sample preparation procedure was applied to selenium tablets: One tablet was weighed and then, it was grinded in mortar to get a powder form of the tablet. The powder was transferred into 100 mL of Teflon flask and then, 70 mL of deionized water was added. It was kept in ultrasonic bath at 40 ºC for 30 minutes. Then, the solution was transferred to 100 mL of volumetric flask (polypropylene). The volume was completed up to mark with deionized water. Then, the solution was filtered through 0.45 μm filter paper. Appropriate volume of filtrate and acetic acid were taken by micropipettes to prepare working solutions (50 μg/L Se (IV)). The optimized acetic acid concentration (0.5 M) was used in working solutions.

Direct calibration curve was drawn by using standard Se (IV) solutions in the concentration range of 20-70 μg/L to determine the concentration of selenium in dietary supplement tablets.

2.6.4. Interference Study

Interference effect of the following elements on Se (IV) signal was studied: antimony (Sb), lead (Pb), copper (Cu), silicon (Si), manganese (Mn), nickel (Ni), calcium (Ca) and aluminum (Al). In these experiments, first, signal of 50 μg/L Se (IV) in 0.5 M acetic acid solution was measured without adding any interfering element. Afterwards, signals of solutions with 1:1, 1:10, 1:50, 1:100, 1:250, 1:500 ratios of Se (IV) : interfering element in 0.5 M acetic acid were measured and then these signals were compared with that of solution of Se (IV).

CHAPTER 3

RESULTS AND DISCUSSION

Within the scope of this thesis, continuous flow photochemical vapor generation tungsten coil atomization technique has been studied. As an analyte, selenium was selected.

The technique was optimized by evaluating the following experimental parameters: trapping and atomization temperatures, flow rates of argon and hydrogen gases, concentration of acetic acid, trapping volume, sample flow rate, irradiation time and type of acid. After determining the optimum value for each parameter, optimization study was repeated one more time.

Tungsten coil was coated with elements having high boiling points to obtain reproducible and sharp signals. It was observed that selenium signal was sharper, more reproducible and sensitive with rhodium coated tungsten coil.

Analytical figures of merit at optimum experimental conditions were reported for selenium using the photochemical vapor generation technique.

Continuous flow photochemical vapor generation tungsten coil atomization technique was applied to selenium dietary supplements to determine selenium concentration in the tablets.

During analyses, it was noticed that the sensitivity of the measurements strongly depended on adjustment of optical path. The optical path was adjusted such that the light beam passes through at the center of the quartz tube atomizer. Moreover, light should pass above the tungsten coil. When these conditions can not be provided, a strong background absorption was observed. The adjustment of the optical path was done before every analysis meticulously.

Last part of this thesis includes interference study. Some serious non-spectral interferences may arise during PVG. Mainly two types of interferences are encountered: liquid phase and gas phase. Liquid phase interference take place in volatile compound generation step. Gas phase interferences can be categorized with respect to the time or place of their occurrence: transport or atomization interferences [63]. For UV-PVG TC-AAS system, interference effect of PVG-amenable elements, transition metals and earth-based elements were studied. It was concluded that source of these interferences arise from both liquid and gas interferences.

3.1. Optimization of Trapping and Atomization Temperatures

The optimization studies were started with the temperature of tungsten coil at trapping and atomization steps. The temperature of tungsten coil was controlled by a variable potential power supply. The temperature vs. voltage correlation was taken from the thesis from Ataman's research group [64,65]. For voltages lower than 2.0 V, Figure 3.1 was used to determine temperatures. For higher voltages, Figure 3.2 was used. Temperature below 1000 °C thermocouple and above 1000 °C pyrometer were used to find the correlation between voltage applied to the coil and the temperature of the coil. Since the sensitivity of the pyrometer is not enough to measure temperature values below 1000 °C.

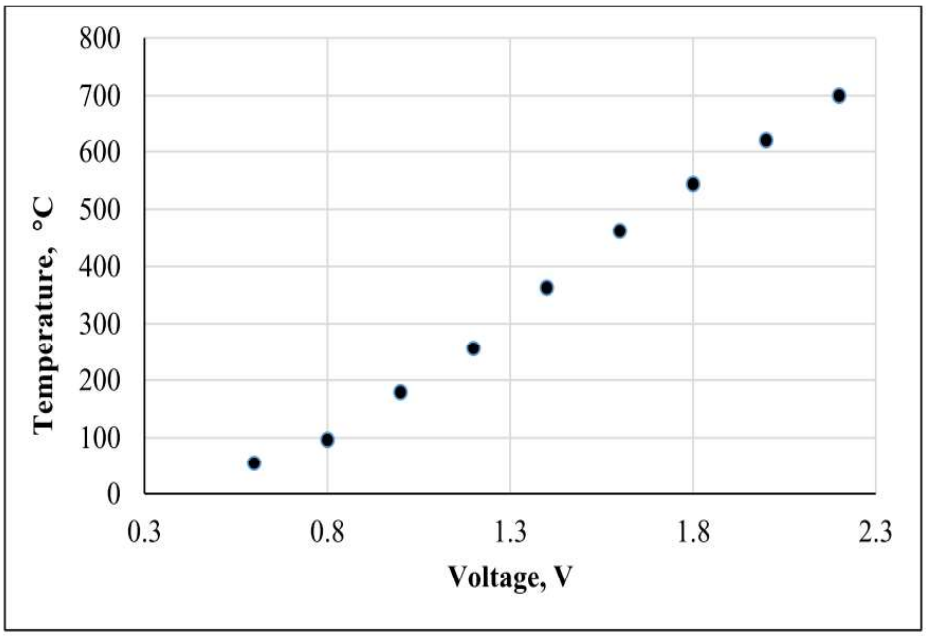

Figure 3.1. Voltage vs. temperature relationship measured by thermocouple [64]

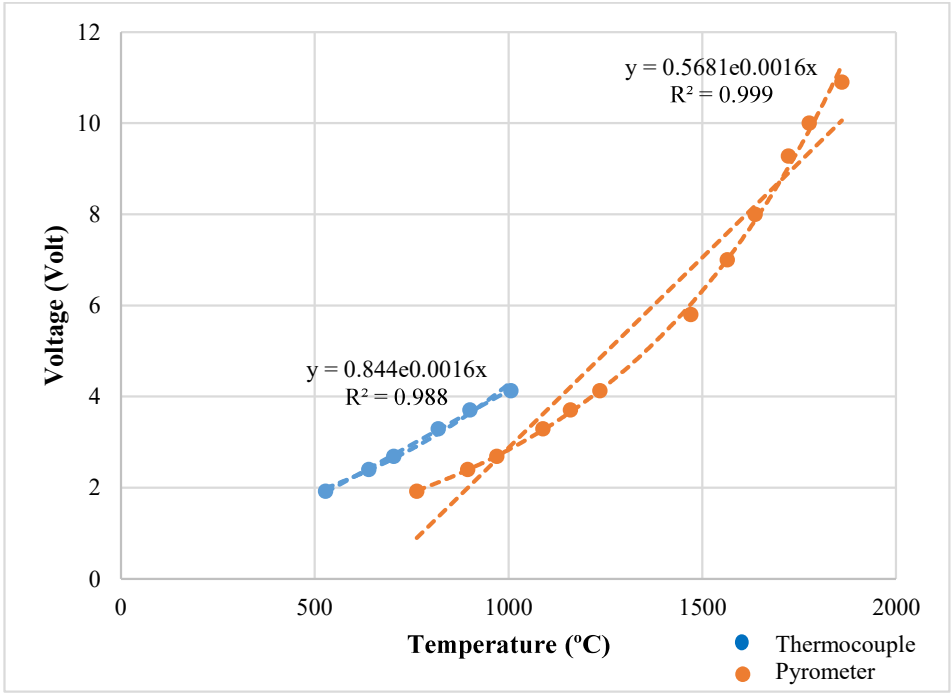

Figure 3.2. Voltage vs. Temperature Relationship measured by thermocouple and pyrometer [65]

The relationship between the absorbance signal and the trapping and atomization temperatures is given in Figure 3.3. The results indicated that the absorbance signal is greatly influenced by the change in trapping and atomization temperatures. During the optimization of trapping temperature, it should be noted that none of the volatile selenium species can remain intact at temperatures as high as 500 ºC. In case of acetic acid, detected volatile specie as a result of irradiation of Se (IV) in acetic acid solution was given as dimethyl selenide in PVG studies [26,30]. Therefore, it can be suggested that after decomposition of the volatile selenium species, free selenium amalgamates with rhodium and tungsten. During this chemical reaction, as the temperature gets higher, possibility of revolatilization from the surface will take place. On the other hand, the temperature should be sufficiently high so that the rate of decomposition and amalgamation on the surface will be optimum. Therefore, at low temperatures these conditions will not be met. The temperature that is sufficiently high to provide best kinetic conditions, but not so high as to cause revolatilization must be found. Trapping temperature was studied between 30 ºC and 793 ºC while atomization temperature kept constant at 1665 ºC. As it can be seen from the Figure 3.3., increasing the trapping temperature up to 643 ºC increased the absorbance signal significantly. Then, as the temperature is increased from 643 ºC, a decrease in the absorbance signal was observed. 643 ºC was selected as an optimum trapping temperature since the maximum absorbance was obtained at that temperature.

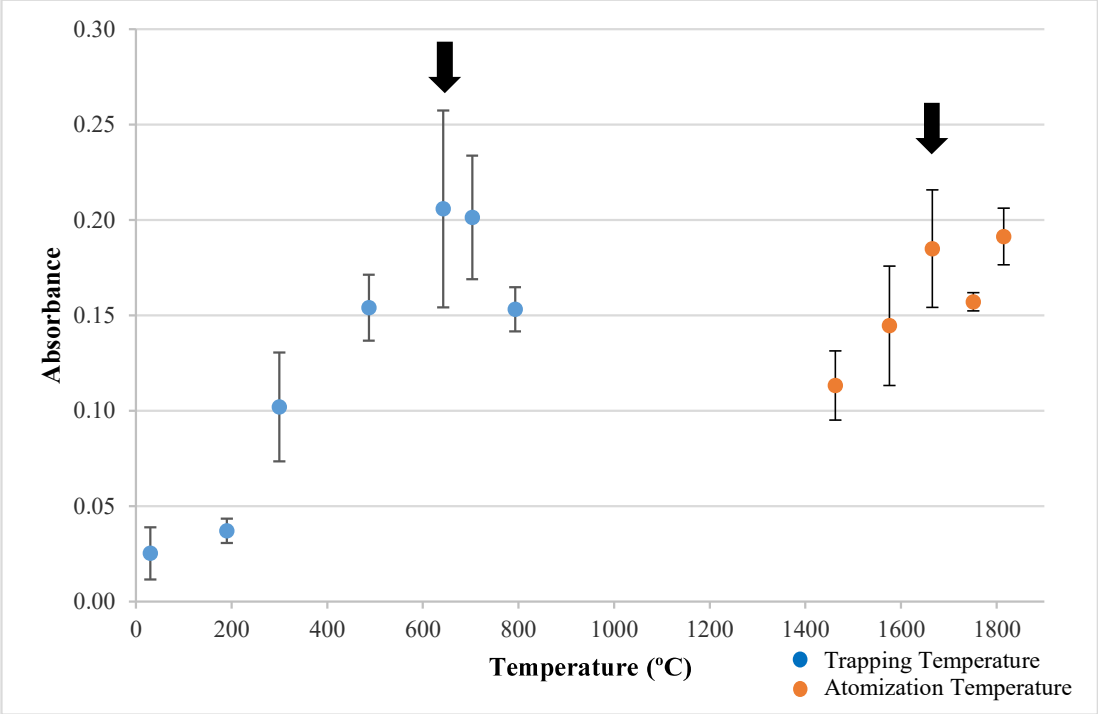

Figure 3.3. Effect of trapping and atomization temperature on the absorbance signal of 50 µg/L Se (IV) in 0.5 M acetic acid solution. Argon flow rate: 200 mL/min, hydrogen flow rate: 400 mL/min, trapping volume: 6.0 mL, trapping period: 45 s, sample solution flow rate: 6.0 mL/min, irradiation time: 2.5 min.

For optimization of the atomization temperature, trapping temperature was kept constant at 643 ºC. The atomization temperature was varied between 1463 ºC and 1815 ºC. When the atomization temperature is increased, absorbance signal increases significantly. As the temperature was increased from 1665 ºC to higher temperatures, the signal remained nearly constant. In order to extend the lifetime of tungsten coil, 1665 ºC was selected as optimum atomization temperature.

Shape of absorbance signals obtained with different trapping temperatures are shown in Figure 3.4. As the trapping temperature is increased, absorbance signal increases. It was also observed that the peak is getting narrower as the temperature increases. A similar phenomenon was more clearly observed with atomization temperature (Figure 3.5). Peak narrowing takes place at high temperatures with change in atomization

temperature. This was an expected result since at lower temperatures, slow rate of analyte release from the surface of the coil causes peak broadening.

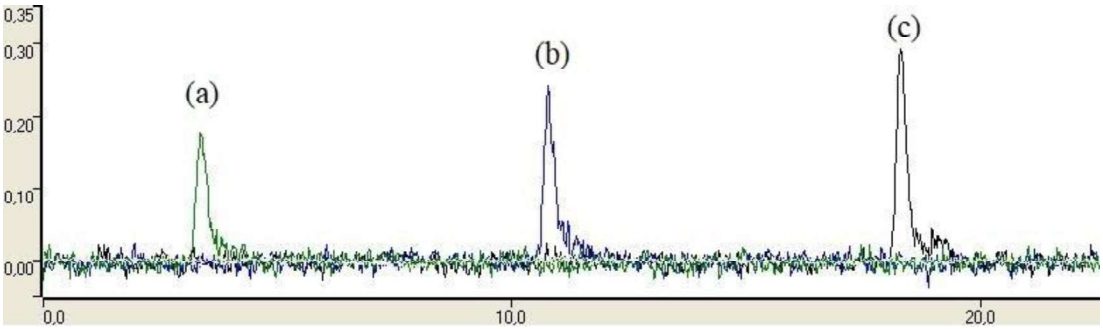

Figure 3.4. The absorbance signals obtained at atomization temperature of 1665 ºC with different trapping temperatures (a) 487 ºC; (b) 643 ºC; (c) 703 ºC.

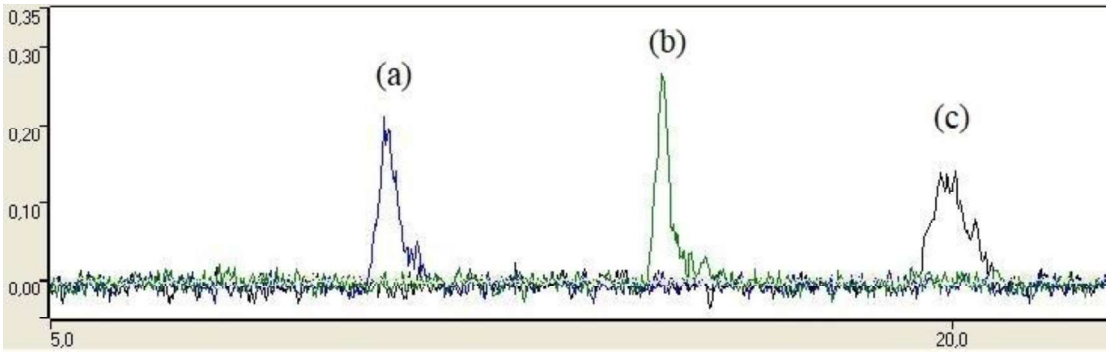

Figure 3.5. The absorbance signals obtained at trapping temperature of 643 ºC with different atomization temperatures: (a) 1575 ºC; (b) 1665 ºC; (c) 1462 ºC.

3.2. Optimization of Argon Flow Rate

The type and flow rate of carrier gas are important factors for PVG since these factors influence both gas-liquid separation process and atomization process in the atomizer [27]. Argon was used as a carrier gas in this study. The use of argon as a carrier gas is desirable because of its inertness. The volatile species generated in the UV-photochemical reactor was carried to gas-liquid separator and tungsten-coil atomizer using argon gas.

The effect of argon flow rate on the absorbance signal of 50 μg/L Se (IV) is shown in Figure 3.6. Argon flow rate was varied from 38 mL/min to 342 mL/min. At low flow rates, a sharp decrease in the analytical signal was observed. This could be attributed to low transport efficiency of the generated volatile species to the atomizer. Between the flow rate of 75 mL/min and 300 mL/min, the absorbance signal remains nearly constant. When the flow rate reaches to 342 mL/min, a significant decrease in the analytical signal was observed. Low analytical signal at high argon flow rate could be explained by the dilution of volatile species in the measurement zone. Moreover, residence time of volatile analyte species are reduced in case of high flow rate of argon. Optimum value of argon flow rate was selected as 200 mL/min for continuous flow photochemical vapor generation tungsten coil atomization technique.

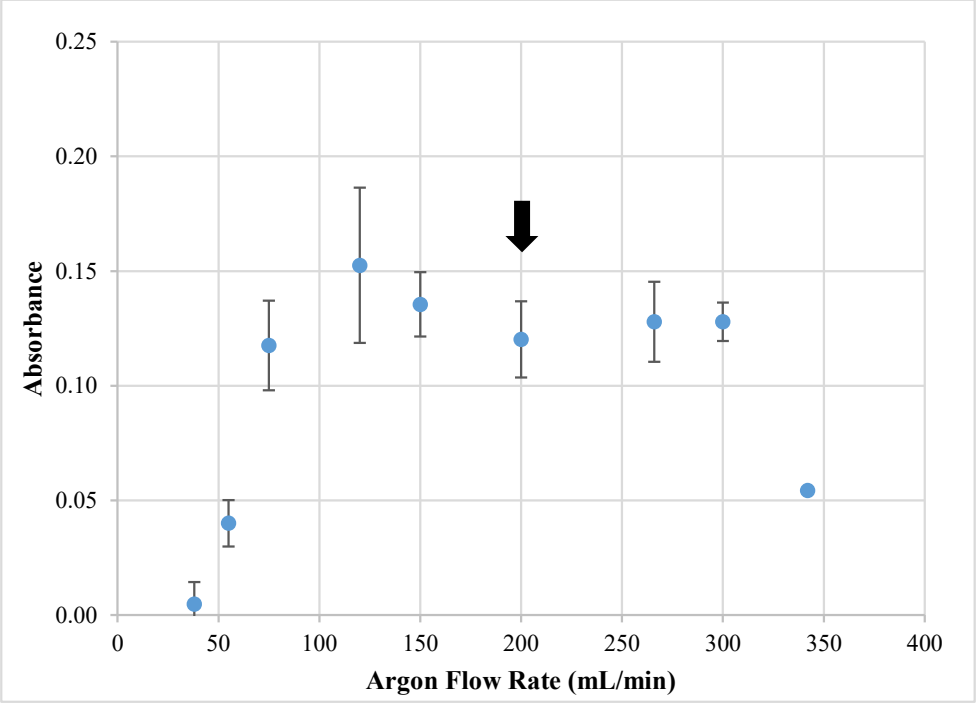

Figure 3.6. Effect of argon flow rate on the absorbance signal of 50 µg/L Se (IV) in 0.5 M acetic acid solution. Trapping temperature: 643ºC, atomization temperature: 1665ºC, hydrogen flow rate: 400 mL/min, trapping volume: 6.0 mL, trapping period: 45 s, sample solution flow rate: 6.0 mL/min, irradiation time: 2.5 min.

3.3. Optimization of Hydrogen Flow Rate

Hydrogen provides not only efficient atomization but also prevent the oxidation of W-coil. Free radical population needed for atomization of volatile species are provided by hydrogen gas as explained in 1.4.1.2.[27]. For this reason, hydrogen is introduced directly to the W-coil atomizer.

The effect of hydrogen flow rate on the analytical signal of selenium is illustrated in Figure 3.7. The flow rate of hydrogen gas was investigated between 80 mL/min and 700 mL/min. The optimum value of hydrogen flow rate was selected as 400 mL/min since reproducible and sharp signal was obtained at this flow rate. Argon flow rate was selected as 200 mL/min. This implies that the hydrogen flow rate is two times that

of argon flow rate. It could be deduced that a reducing environment is necessary for the atomization of volatile selenium species.

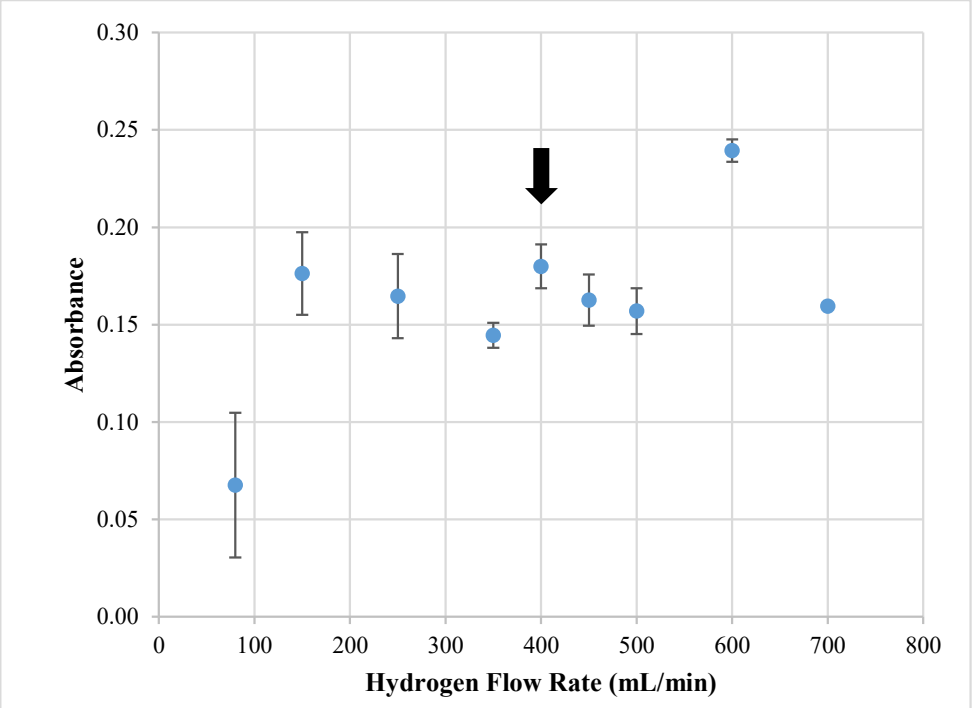

Figure 3.7. Effect of hydrogen flow rate on the absorbance signal of 50 µg/L Se (IV) in 0.5 M acetic acid solution. Trapping temperature: 643 ºC, atomization temperature: 1665 ºC argon flow rate: 200 mL/min, trapping volume: 6.0 mL, trapping period: 45 s, sample solution flow rate: 6.0 mL, irradiation time: 2.5 min.

3.4. Optimization of Concentration of Acetic Acid

The efficiency of photochemical vapor generation technique strongly depends on the presence of organic photochemical agents in the solution. In this study, acetic acid was used to react with Se (IV) to produce volatile selenium species under UV irradiation.

Figure 3.8. shows the effect of sample flow rate on absorbance signal of 50 µg/L Se (IV). In the concentration range of 0.25 to 2.0 M, the optimum acetic acid

concentration was investigated. The highest absorbance signal was measured at 0.5 M acetic acid. It was selected as optimum acetic acid concentration. At higher acetic acid concentrations, a decrease in absorbance signal was observed. This result could be attributed to mechanism of PVG of selenium in the presence of acetic acid. Guo and coworkers suggested that methyl and carboxyl radicals are generated as a result of irradiation of acetic acid solution [27,38]. Higher acetic acid concentration could lead to generation of large number of reducing radicals in the medium which results in decreasing efficiency of PVG reactions.

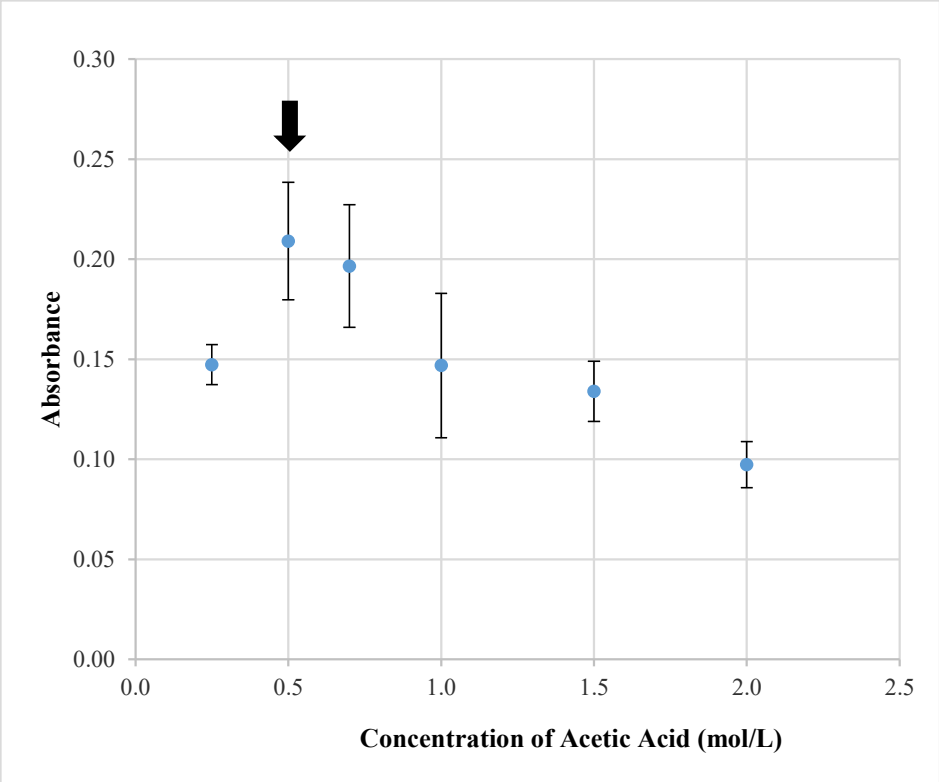

Figure 3.8. Effect of acetic acid concentration on the absorbance signal of 50 µg/L Se (IV). Trapping temperature: 643 ºC, atomization temperature: 1665 ºC argon flow rate: 200 mL/min, hydrogen flow rate: 400 mL/min, trapping volume: 6.0 mL, trapping period: 45 s, sample solution flow rate: 6.0 mL, irradiation time: 2.5 min.

3.5. Optimization of Sample Flow Rate

In this study, solutions containing selenium and acetic acid was introduced to UV-photochemical reactor by a peristaltic pump. Flow rate of the solution affects the UV-light exposure time of the solution. To investigate the influence of sample flow rate on the analytical signal, total volume of the sample was kept constant at 6.0 mL which was introduced to the UV-PVG W-coil trap atomization system with different flow rates. As the sample flow rate is decreased, trapping period is increased because it takes longer time solution reaching to the coil. Trapping periods were set to 180 s, 60 s, 45 s and 30 s for the sample flow rates of 1.75 mL/min, 4.0 mL/min, 6.0 mL/min and 8.0 mL/min, respectively. It is noteworthy that after the sample solution reaches to end of photoreactor, argon gas speeds up the sample flow rate. As a result, trapping period decreases than expected. For instance, when the solution is pumped for 60 s at 6 mL/min, the expected trapping period of 60 s decreased to 45 s.

Figure 3.9. demonstrates the effect of sample flow rate on absorbance signal of 50 μg/L Se (IV) in 0.5 M acetic acid solution. When the sample solution flow rate was increased from 1.75 mL/min to 4.0 mL/min, two times increase in the absorbance signal was measured. Low absorbance signal at 1.75 mL/min flow rate could be caused by long trapping period (180 s). An efficient trapping might not be achieved because of sweeping of volatile species from atomizer in this time period. The absorbance remained constant when the sample flow rate was increased to 6.0 mL/min. A slight decrease in the signal was observed when 8.0 mL/min sample flow rate was used. As an optimum flow rate of sample solutions, 6.0 mL/min was selected.

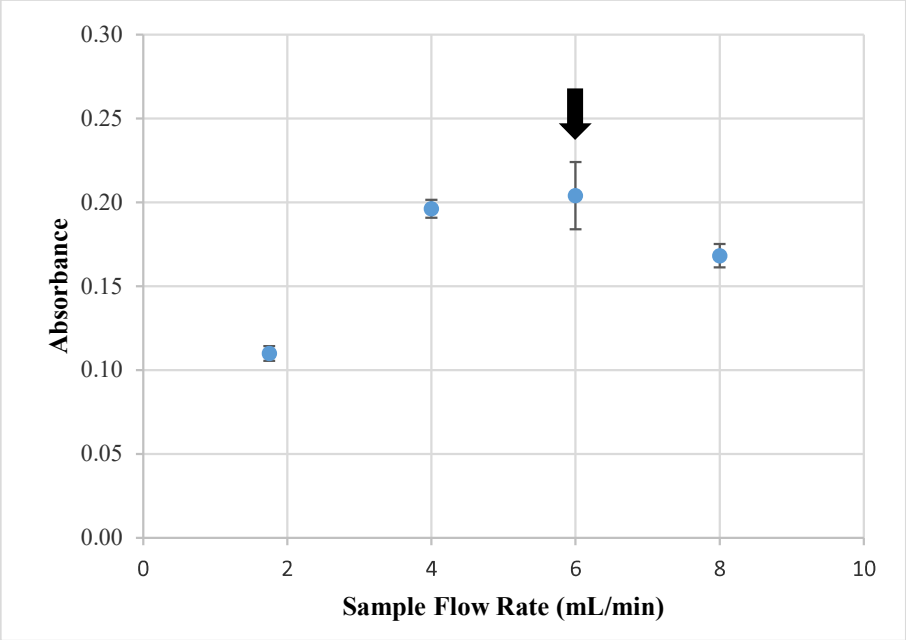

Figure 3.9. Effect of sample flow rate on absorbance signal of 50 µg/L Se (IV) in 0.5 M acetic acid solution. Trapping temperature: 643 ºC, atomization temperature: 1665 ºC, argon flow rate: 200 mL/min, hydrogen flow rate: 400 mL/min, trapping volume: 6.0 mL, irradiation time: 2.5 min.

3.6. Optimization of Trapping Volume

The trapping volume used in one measurement was optimized. The relationship between absorbance signal and trapping volume is shown in Figure 3.10. As the trap volume increases, absorbance signal increases linearly. This is an expected result since total mass of analyte trapped on W-coil increases as trap volume increases. When the trapping volume is increased, trapping time also increases. 6.0 mL was used as a sample volume and trap time was used as 45 s. 6.0 mL was selected as optimum value for trapping volume and it was used throughout the study.

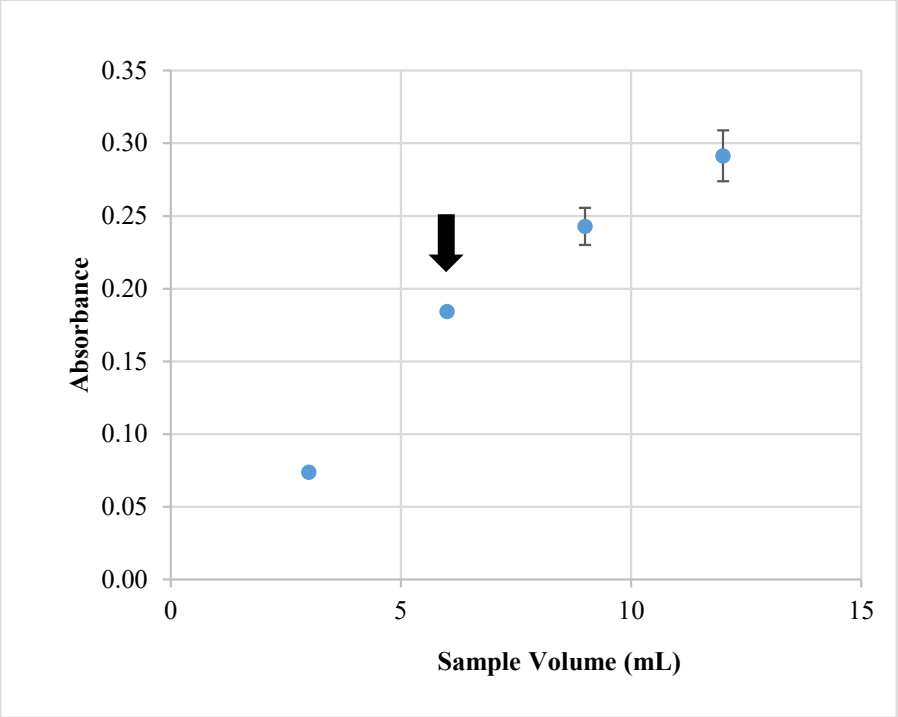

*Figure 3.10. E*ffect of sample volume on absorbance signal of 50 µg/L Se (IV) in 0.5 M acetic acid solution. Trapping temperature: 643 ºC, atomization temperature: 1665 ºC argon flow rate: 200 mL/min, hydrogen flow rate: 400 mL/min, sample solution flow rate: 6.0 mL, irradiation time: 2.5 minutes.

3.7. Optimization of Irradiation Time

Irradiation time is an important parameter since it affects the exposure time of solution to UV-light. The length of UV-lamp used in the study was 43.6 cm. When this lamp was wrapped with a FEP tubing and 6.0 mL/min sample flow rate was used, time from solution enters into the lamp and leaves from the lamp was measured as 2.5 minutes.

To investigate the effect of irradiation time on absorbance signal, the solution was kept in the photochemical reactor for longer times. Figure 3.11 gives the relation of irradiation time with absorbance signal. As it can be seen, a slight increase in the signal was observed as the irradiation time increased. Then, the signal start decreasing. To keep the analysis time as short as possible, 2.5 minutes of irradiation time in which

the solution flows through continuously without any delay, was selected as optimum irradiation time.

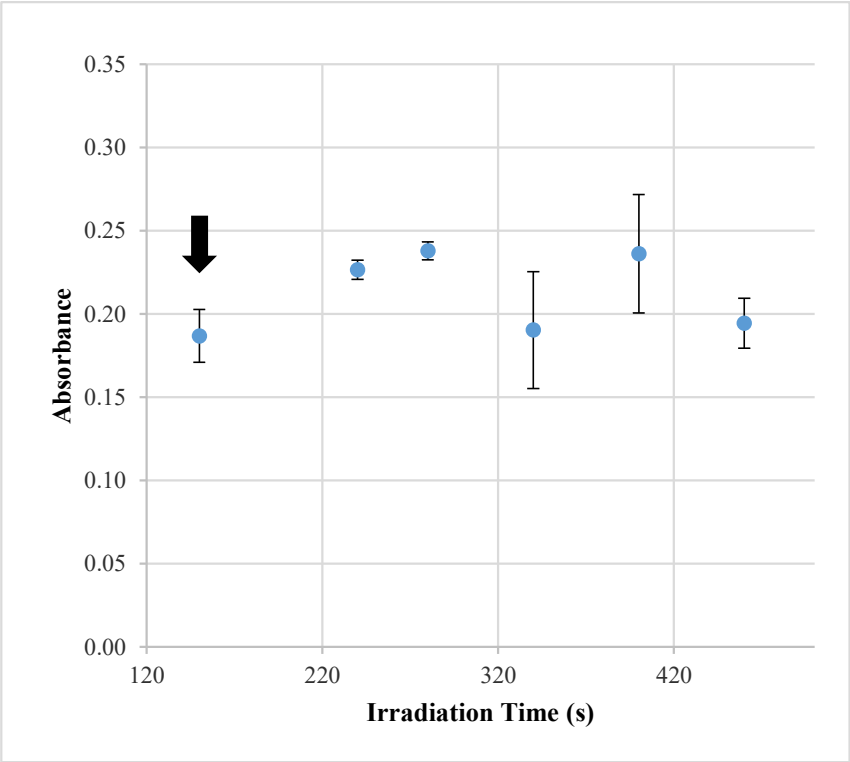

Figure 3.11. Effect of irradiation time on absorbance signal of 50 µg/L Se (IV) in 0.5 M acetic acid solution. Trapping temperature: 643 ºC, atomization temperature: 1665 ºC argon flow rate: 200 mL/min, hydrogen flow rate: 400 mL/min, trapping volume: 6.0 mL, trapping period: 45 s, sample solution flow rate: 6.0 mL/min.

3.8. Coating of Tungsten Coil

In GFAAS, chemical modification have been used since the establishment of stabilized temperature platform furnace (STPF). A chemical modifier is a concentrated solution containing one or more chemical compounds capable of stabilizing the analyte and promoting matrix removal by volatilization in pyrolysis

step [66]. This strategy enables working at higher temperatures, which results in improved accuracy and precision. Background signal and potential interferences are also minimized [67].

Chemical modification was implemented to tungsten coil atomizer in many studies. For instance, ammonium dihydrogen phosphate ($NH_4H_2PO_4$) [68], ascorbic acid [69] and a mixture of Pd and Mg [70] was used as chemical modifiers. Similar to graphite furnace AAS, thermal stabilization of analytes is promoted by these compounds. Later, Silva and coworkers proposed a different strategy for chemical modification. They reported that by supporting gas phase reactions between the modifier and analyte species, sensitivity and precision were improved for Cr and Sr. It was suggested that the sensitivity improvements derived from gas phase reactions containing charge transfer [67].

In this study, to improve trapping efficiency, coating process was applied. The surface of the tungsten coil can be coated with elements having high boiling points. This requirement is needed to prevent loss of material from the surface of the coil.

Signals obtained with bare tungsten coil was not reproducible. Then, rhodium (Rh), iridium (Ir), ruthenium (Ru), palladium (Pd) and cobalt (Co) were investigated to be used as coating element for W-coil. For coating procedure, the same temperature program was used for all elements.

Figure 3.12 demonstrates effect of coating element on the absorbance signal of selenium. Among these elements, the most sensitive, a sharp, and reproducible signal was obtained with rhodium (Rh) coated W-coil. It was selected as the optimum coating element. All the optimization studies were carried out with Rh coated tungsten coil. Before each set of experiment, absorbance signal of 50 μg/L Se (IV) was measured and if there is a decrease in the absorbance signal the coil was replaced with a new Rh coated W-coil. One Rh coated W-coil was used nearly 500 firings.

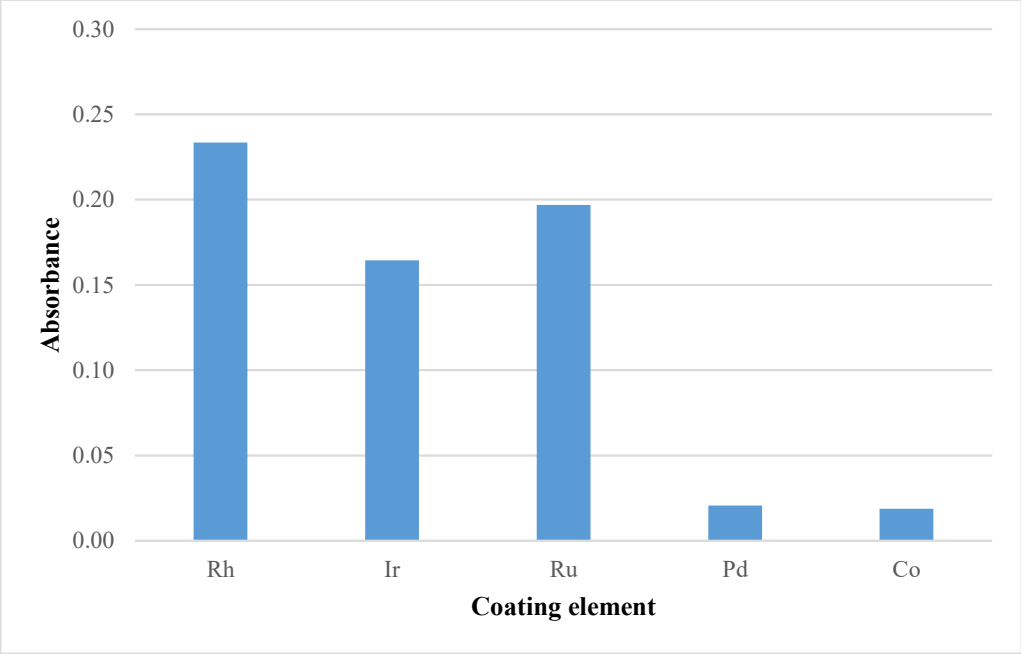

Figure 3.12 . Effect of coating element on absorbance signal of 50 µg/L Se (IV) in 0.5 M acetic acid solution. Trapping temperature: 643 ºC, atomization temperature: 1665 ºC argon flow rate: 200 mL/min, hydrogen flow rate: 400 mL/min, trapping volume: 6.0 mL, trapping period: 45 s, sample solution flow rate: 6.0 mL/min.

3.9. Type of Organic Acid

In UV-PVG, low molecular weight (LMW) organic acids such as formic acid, acetic acid, propionic acid and malonic acid have been used to obtain volatile analyte species in literature [24]. Absorption of UV radiation by low molecular weight organic acids results in formation of reducing radicals in the sample solution [24].

In this study, the preliminary studies of PVG system was performed by using formic acid. Since no analytical signal was measured with UV-PVG of selenium in formic acid solutions, the studies were continued with acetic acid. First successful results were obtained with acetic acid solutions. Then, the remaining analyses was performed by using acetic acid.

After the optimization of parameters was completed, continuous flow photochemical vapor generation tungsten coil atomization technique was used to analyze selenium solutions in formic acid and propionic acid. Acid concentration range was from 0.5 to 2.0 M. No absorbance signal different than that of blank solutions was obtained from formic acid or propionic acid. This could be attributed to the length of reaction coil. In the literature, it was stated that the required length of reaction coil depends on the type of organic acid [42,43]. Rybinova and coworkers reported that the length of reaction coil required for the UV-PVG process of the acetic acid was found to be three times larger than that required for formic acid [42]. Figueroa and coworkers explained this with photoreduction kinetics. With the lowest molecular weight organic acids, photoreduction kinetics are faster[71]. Photolysis of formic acid yields to H_2, CO and CO_2 end products while higher order carboxylic acid such as acetic and propionic acid yields to CH_3 and C_2H_5 radicals[24]. Longer reaction times are needed for the formation of CH_3 and C_2H_5 radicals. In our system the length of the coil is 50 m. This is the maximum length which is limited to the length of the lamp (43.6 cm) and also the diameter of the FEP tubing (O.D.:4.0 mm, I.D.:2.5 mm). Thus, for formic acid, the length of the reaction coil used in this study (50 m) could be a reason for not obtaining an absorbance signal from selenium solutions in formic acid. It was also stated that long reaction coil can lead to loss of analyte due to undesirable photochemical decompositions [43]. On the other hand, for propionic acid, the length of reaction coil probably was not sufficient for the formation of C_2H_5 radicals.

Optimized parameters of UV-PVG TCAAS system is summarized in Table 3.1.

Table 3.1. Optimized Parameters for UV-PVG TCAAS

Parameter	Optimum Value
Trapping Temperature	643 ºC
Atomization Temperature	1665 ºC
Argon Flow Rate	200 mL/min
Hydrogen Flow Rate	400 mL/min
Concentration of Acetic Acid	0.5 mol/L
Sample Flow Rate	6.0 mL/min
Irradiation Time	2.5 min
Trapping Volume	6.0 mL
Trapping Period	45 s

3.10. Analytical Figures of Merit

The calibration plot was obtained for Se (IV) standard solutions in the concentration range from 20 µg/L to 110 µg/L. It was observed that the calibration plot is linear in the range of 20 µg/L to 70 µg/L. After 70 µg/L, a deviation from linearity was detected. The best line equation obtained for the calibration plot and correlation coefficient were obtained as $y = 0.0049x - 0.0421$ and 0.9992, respectively. (x is Se (IV) concentration in µg/L and y is the absorbance value)

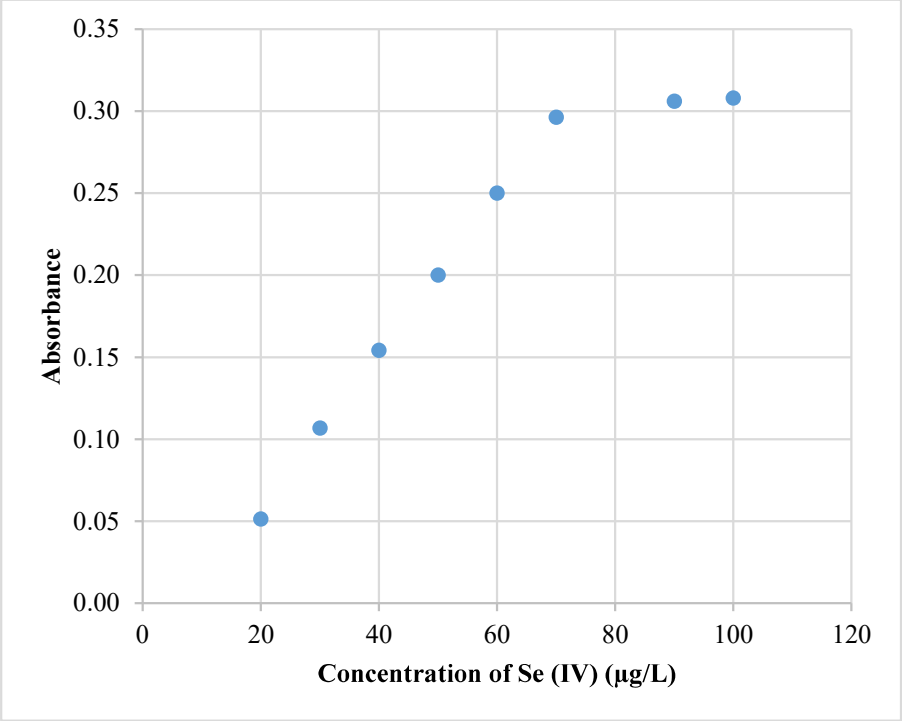

Figure 3.13. Calibration plot of Se (IV) in 0.5 M acetic acid solution.

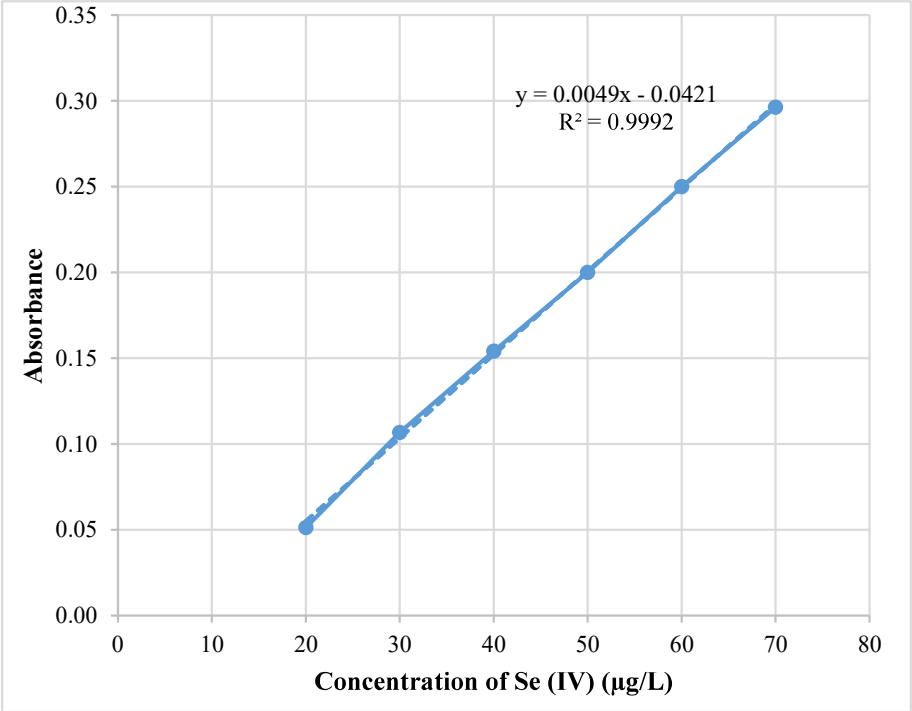

Figure 3.14. Linear range of calibration plot for Se (IV)

Analytical figures of merit for CF-PVG W-coil AAS technique is given in Table 3.2. Limit of detection, limit of quantification and RSD % values were calculated from 8 replicate measurements of blank solution. LOD and LOQ were determined as 3.3 μg/L and 11.1 μg/L respectively. It should be noted that Se (IV) solutions below the concentration of 20 μg/mL could not be detected because of negative intercept of calibration plot.

LOD of current method was compared with that of other methods proposed in the literature. The value is comparable with early application of PVG. For example, in the first application of PVG where quartz tube atomizer was used, LOD was given as 2.5 μg/L [27]. Then, improved limit of detections were obtained by other groups using different atomizers such as argon-hydrogen flame with preconcentration [41] (0.0008 μg/L), graphite tube atomizer [42] (4.1 ng/L), miniature diffusion flame [30] (0.10 μg/L) etc. Thus, LOD of current method is not competitive with these studies.

Table 3.2. *Analytical Figures of Merit for CF-PVG W-coil AAS Technique*

Analytical Figures of Merit	
Limit of Detection, LOD (3s/m n=8), μg/L	3.3
Limit of Quantification, LOQ (10s/m) n=8, μg/L	11.1
Dynamic Range, μg/L	11-70
RSD %	14.0

3.11. Determination of Se (IV) in Selenium Dietary Supplements by CF-PVG W-Coil Atomization AAS

Continuous flow photochemical vapor generation tungsten-coil atomization AAS technique was used to analyze selenium dietary supplements. Selenium tablets containing sodium selenite (Na_2SeO_3) was selected since the method is optimized for Se (IV). The tablets contain microcrystalline cellulose and lactose monohydrate besides sodium selenite.

Sample solutions were prepared in three replicates. Randomly selected three tablets were weighed and then dissolved in in deionized water using ultrasonic shaker. Each replicate was diluted with deionized water so that the final concentration of Se (IV) would be 50 µg/L.

Direct calibration plot was used to determine the selenium concentration in the tablets. Mean concentration of Se (IV) in three replicates of the tablet was found to be 193.4 µg ± 5.3%. Selenium mass in one tablet is reported as 200 µg by the manufacturer. t-test was applied between the concentration result obtained in this study and the reported value and no significant difference is found between two concentration values at 95 % confidence level. According to regulation of European Commission Health and Consumers Directorate, deviations from declared content up to +45/−20% is tolerated for minerals in food supplements. Moreover, food supplements are not subjected to restrict quality control as pharmaceutical products.

3.12. Interference Study

One of the attractive features frequently attributed to PVG is the reduction in interference from elements compared to those experienced by conventional CVG. However, because of its reducing mechanism, interferences arise from transition metals (Cu, Fe, Ni, Co) and common oxidants (dissolved oxygen, nitrate and nitrite ions). It was reported that transition metals show both suppressing and enhancing effects on photochemically generated analytes whereas common oxidants are always suppressive [24].

Non-spectral interferences cause an effect on the number of analyte atoms in absorption volume and consequently, on the signal. They can be categorized with respect to the time or place of their occurrence. To illustrate, when the determination of analyte is carried out as a result of a chemical reaction such as HGAAS, CVAAS, PVG; liquid phase interferences may come up [12]. Gas phase interferences are another type of interferences. For instance, transport interferences arise when volatile species are transported to atomizer. This type of interference could cause a delay on the transportation of the analyte or loss of volatile analyte species [72]. Lastly, atomization interferences are caused by change in the fraction of the analyte that is dissociated, excited, or ionized in the vapor phase [12].

In this study, the interferences were studied in three different groups. First group involves elements amenable to photochemical vapor generation (Sb, Pb). Second group of elements consist of transition metals (Mn, Ni, Cu, Co). The third group comprise of earth-based elements (Al, Ca, Si, Na).

3.12.1. Interference of Elements Amenable to PVG

For the interference study of elements prone to PVG, antimony (Sb) and lead (Pb) were studied. Other elements like tellurium (Te) and tin (Sn) was not included since the compounds containing these elements need hydrochloric acid solutions to be dissolved. In our studies it was observed that even 0.025 M hydrochloric acid leads to three times decrease in the analytical signal of Se (IV). For this reason, elements in

deionized water or nitric acid solutions were used in the interference study. The interference of hydrochloric acid on PVG has been reported by Zheng and coworkers in a study of determination of mercury [28]. They stated that as the hydrochloric acid (HCl) concentration increased, the efficiency of PVG decreased. To find out whether this effect derived from H^+ or Cl^-, they also studied the effect of sodium chloride (NaCl). They observed a 10% increase in the signal until concentration of 3 mol/L NaCl. At higher Cl^- concentration, the signal starts to decline. It was attributed to complex formation of Cl^- with Hg^{2+}. They also stated that although redox potential of mercury ions are independent of H^+, that of formic acid is dependent of H^+. It was deduced that the effect of hydrochloric acid is caused by combined effect of H^+ and Cl^-. For selenium, the situation might be similar.

It was reported by Zheng and coworkers that UV-PVG is applicable for the determination of antimony Sb (III) [65]. In another study, Gao and coworkers reported determination of Sb (III) and Sb (V) in natural waters by photochemical vapor generation coupled with ICP-MS[66]. In this thesis study, interference effect of antimony is investigated for Sb (III).

Interference effect of antimony is illustrated in Figure 3.15. The solutions were prepared such that concentration of Sb was 1, 10, 50 and 500 times that of the concentration of Se. Until ten times of the analyte concentration, no significant difference on the absorbance was observed. When the concentration of antimony was 500 times of selenium concentration, the signal decreased to 56 %.

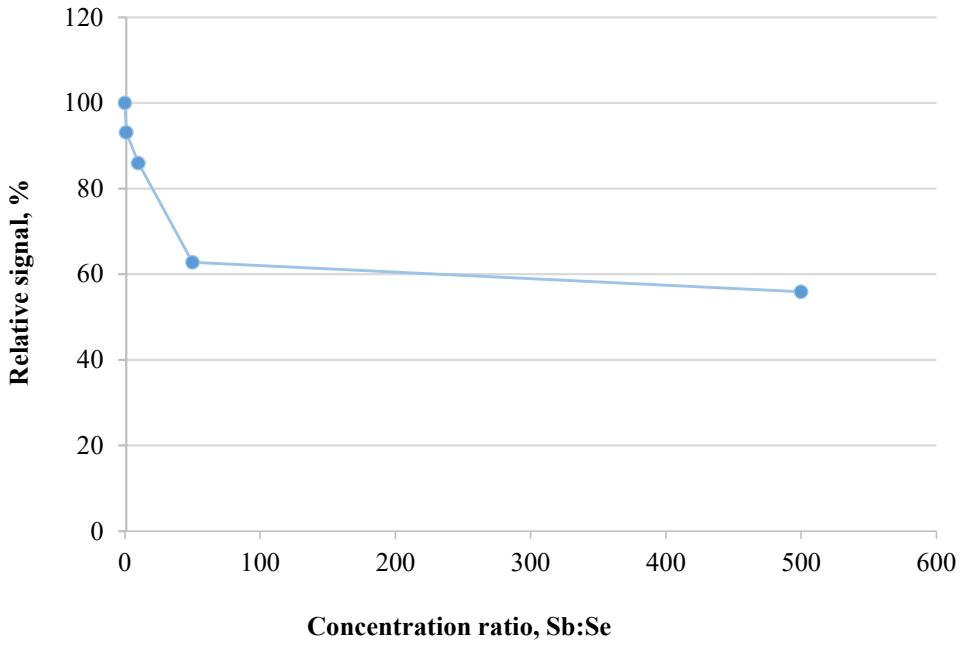

Figure 3.15. Interference effect of antimony on absorbance signal of 50 µg/L Se (IV) in 0.5 M acetic *acid. T*rapping temperature: 643 ºC, atomization temperature: 1665 ºC argon flow rate: 200 mL/min, hydrogen flow rate: 400 mL/min, trapping volume: 6.0 mL, trapping period: 45 s, sample solution flow rate: 6.0 mL/min.

PVG of lead (Pb) was reported by Duan and coworkers [73]. In the solution of 0.90% (v/v) acetic acid, signal of volatile lead species were successfully measured with ICP-MS [73]. Interference effect of lead (Pb) was investigated in this study because of its tendency to form volatile Pb species in acetic acid solution. Interference effect of lead is illustrated in Figure 3.16. A serious interfering effect of lead was observed. When the concentration of lead is only 10 times of selenium concentration, the signal decreased to 30 % therefore, larger concentration of Pb was not further followed.

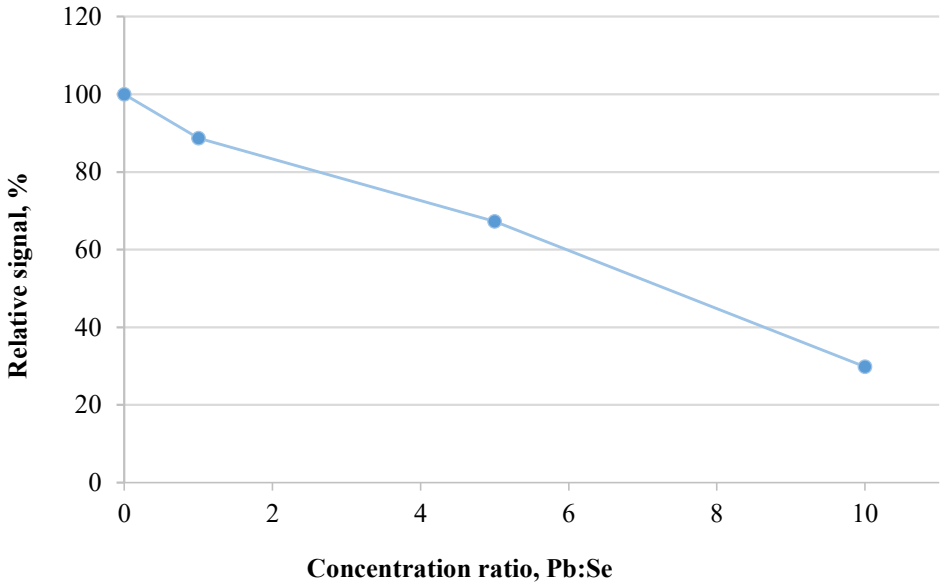

Figure 3.16. Interference effect of lead on absorbance signal of 50 µg/L Se (IV) in 0.5 M acetic acid. Trapping temperature: 643 ºC, atomization temperature: 1665 ºC argon flow rate: 200 mL/min, hydrogen flow rate: 400 mL/min, trapping volume: 6.0 mL, trapping period: 45 s, sample solution flow rate: 6.0 mL/min.

3.12.2. Interference of Transition Metals

Transition metals have both suppressive and enhancive effect on PVG of analytes. Suppressive effect of transition metal might arise since such metal ion can act as an oxidizing agent. Therefore, analyte reduction reactions can be inhibited by depleting the number of reducing radicals in the medium. On the other hand, enhancive effect might result from possible concurrent role of metal as sensitizer for accelerated photo-oxidation of carboxylic acids[24]. For instance, it was reported that Fe (III) increases the oxidation rate of formic acid 100 times faster than it does that of acetic acid [74].

Interference effect of Mn, Ni and Cu were studied for the investigation of interference effect of transition metals to the signal of selenium. Interference effect of manganese (Mn) on the absorbance signal of Se (IV) in 0.5 M acetic acid is shown in Figure 3.17. As the concentration of Mn increases, suppressive effect on the signal of selenium was

observed as seen in the figure however the decrease in the analyte signal is not as big as seen in that of Pb.

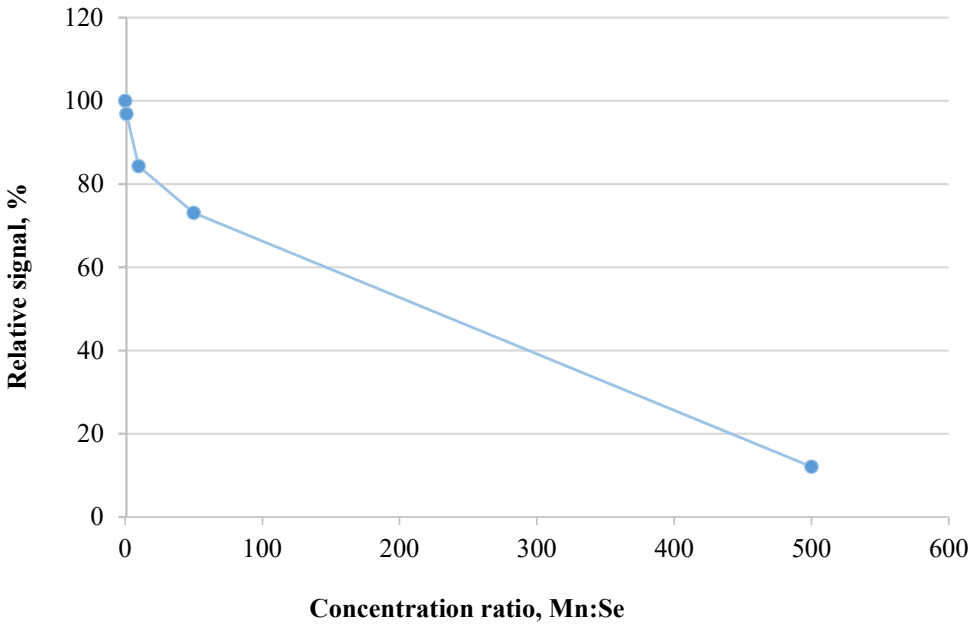

Figure 3.17. Interference effect of manganese on absorbance signal of 50 µg/L Se (IV) in 0.5 M acetic acid. Trapping temperature: 643 ºC, atomization temperature: 1665 ºC argon flow rate: 200 mL/min, hydrogen flow rate: 400 mL/min, trapping volume: 6.0 mL, trapping period: 45 s, sample solution flow rate: 6.0 mL/min.

Interference effect of nickel (Ni) on the absorbance signal of Se (IV) in 0.5 M acetic acid is shown in Figure 3.18. Similar interference effect as followed with the addition of Mn was obtained. At 50-fold concentration of Ni, the relative signal was found to be 73 %. When the concentration of Ni was 500-fold, dramatic decrease in the % relative signal of selenium was obtained.

Guo and coworkers stated that no serious interference effect was observed from nickel on the absorbance signal of Se (IV) determined by PVG [26]. It was stated that up to concentration of 500 mg/L nickel, interference effect was not observed. On the other hand, Campanella and coworkers reported greater influences of nickel. They observed

that 10 mg/L nickel caused 50% decrease on the signal of selenium. In our study, 5 mg/L nickel decreased selenium signal to 73%. Thus, our finding is in accord with Campanella and coworkers's result. It is noteworthy that the interference of elements depend on photo-reactors which effect the reaction temperature and available photon flux. The type and concentration of organic acid are other parameters. Thus, the contradictory results in the literature are derived from these differences [24].

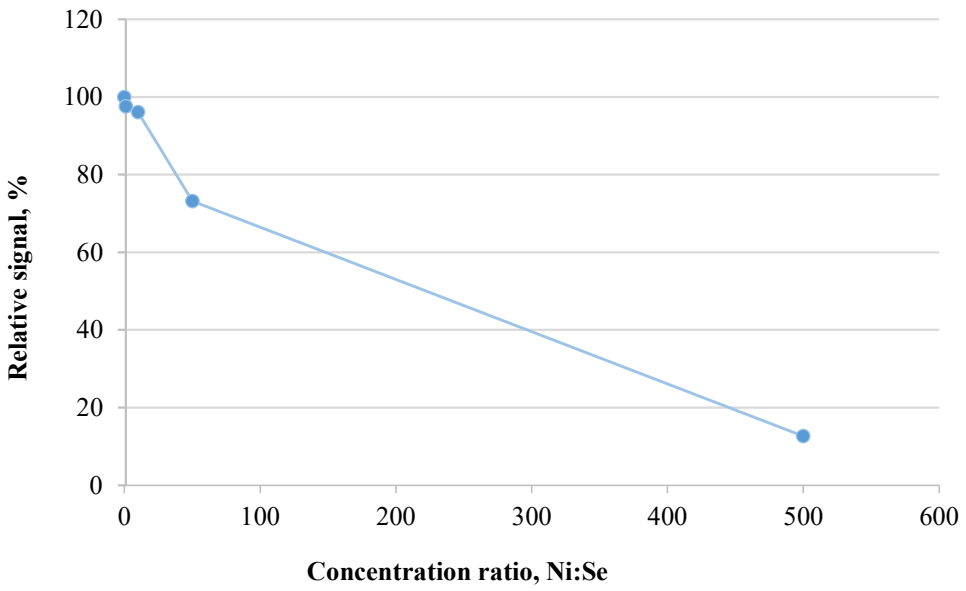

Figure 3.18. Interference effect of nickel on absorbance signal of 50 µg/L Se (IV) in 0.5 M acetic acid. Trapping temperature: 643 ºC, atomization temperature: 1665 ºC argon flow rate: 200 mL/min, hydrogen flow rate: 400 mL/min, trapping volume: 6.0 mL, trapping period: 45 s, sample solution flow rate: 6.0 mL/min.

Interference effect of copper (Cu) on the absorbance signal of Se (IV) in 0.5 M acetic acid is illustrated in Figure 3.19. Much more severe effect compared to that of Mn and Ni was observed in the presence of Cu. When the concentration ratio of Se:Cu was even 1:1, a significant decrease was observed as seen in Figure 3.19. This result is consistent with that of in the literature. For example, in a study where in situ photogeneration of Se volatile compounds were used to determine selenium by

ETAAS, strong depressive effect of Cu was observed. It was stated that when interference to selenium concentration ratio was 1:1, recovery of selenium was determined as 21%. When this ratio is increased to 10:1, recovery decreased to 6% [71]. To prevent this interference, they suggested to add chelating agent such as EDTA to the solution before UV irradiation. Strong interference effect of Cu was also obtained by Guo and coworkers for Se (IV) determined by PVG in acetic acid solution [26]. It was stated that when 200 µg/L of Cu is present in the analyte solution, absorbance signal of 100 µg/L of Se(IV) in 0.7 M acetic acid decreased by 50 % [27]. In another study, PVG of selenium by AFS carried out by Campanella and coworkers, low tolerance to Cu was stated. It was reported that for concentrations higher than 3.0 mg/L of Cu(II), the AFS signal was significantly affected and the recovery was lower than 20%. They attributed this effect to the formation of metallic Cu (0), which gives a heterophasic system in the reaction coil [30]. Another explanation for severe interference effect of Cu was suggested by Sturgeon's review paper [24] on PVG based on Bideau and coworkers's findings [74]. It was stated that Cu, Ni and Fe can change the photoabsorption spectrum of the sample and alter the kinetics of decarboxylation reactions. Even the products of the reaction can be changed by these transition metals. For instance, by LMCT processes, Fe (III) might promote production of OH radicals which consequently change the cascade of reactions leading to CO_2^- [24].

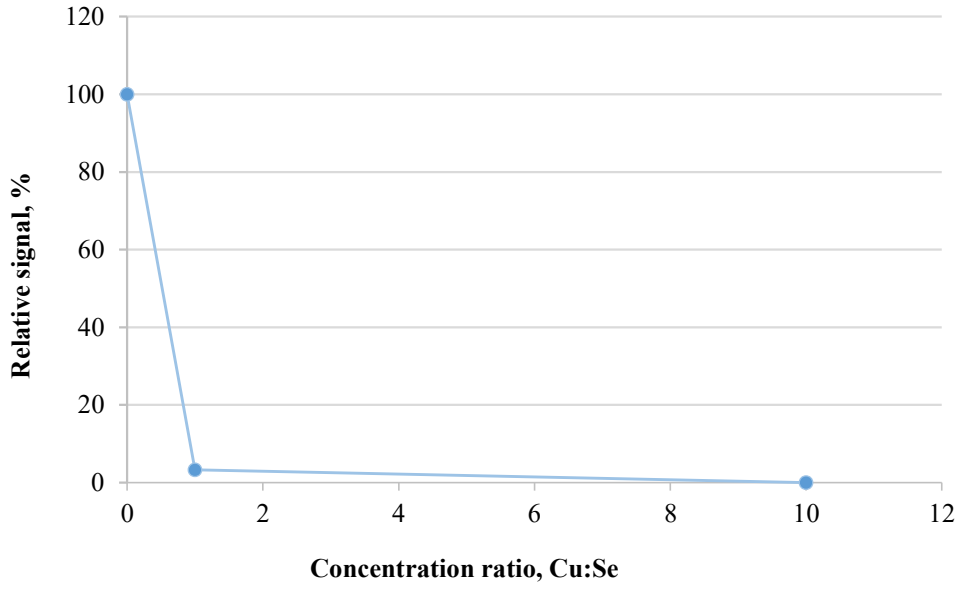

Figure 3.19. Interference effect of copper on absorbance signal of 50 µg/L Se (IV) in 0.5 M acetic acid. Trapping temperature: 643 ºC, atomization temperature: 1665 ºC argon flow rate: 200 mL/min, hydrogen flow rate: 400 mL/min, trapping volume: 6.0 mL, trapping period: 45 s, sample solution flow rate: 6.0 mL/min.

Interference effect of cobalt on absorbance signal of Se (IV) is illustrated in Figure 3.20. When the concentration ratio of Co:Se was 1:1, relative signal of the solution was detected as 81%. When this ratio is increased to 10:1, the signal increased to 98%. On the other hand, a sudden decrease was observed in the absorbance signal of Se (IV) when Co:Se concentration ratio was 50:1. This result can be attributed to generation of cobalt carbonyl in the medium. Grinberg and coworkers reported generation of volatile cobalt species by UV photoreduction [37]. As a result of UV irradiation in the presence of acetic acid, volatile cobalt species might have generated. This could lead to decrease in the absorbance signal of Se (IV).

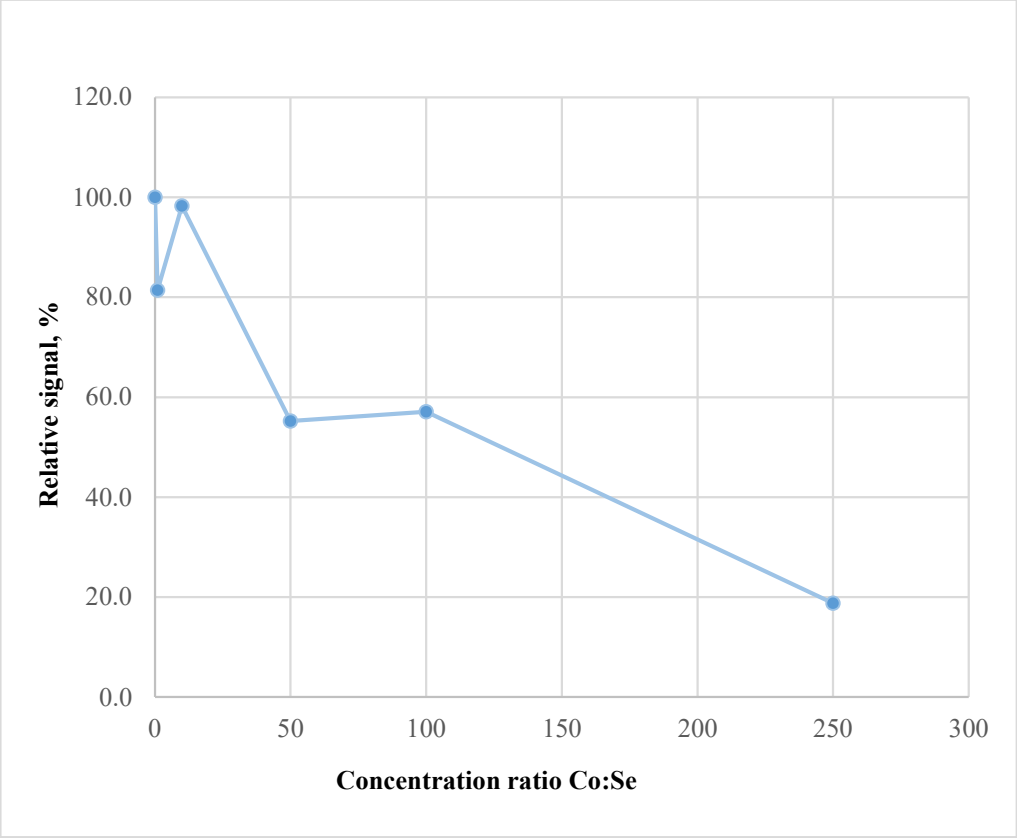

Figure 3.20. Interference effect of cobalt on absorbance signal of 50 µg/L Se (IV) in 0.5 M acetic acid. Trapping temperature: 643 ºC, atomization temperature: 1665 ºC argon flow rate: 200 mL/min, hydrogen flow rate: 400 mL/min, trapping volume: 6.0 mL, trapping period: 45 s, sample solution flow rate: 6.0 mL/min.

3.12.3. Interference of Earth-Based Elements

The last group of interfering elements were selected among earth-based elements. Aluminum (Al), calcium (Ca) and silicon (Si) were studied.

Interference effect of calcium (Ca), aluminum (Al), silicon (Si) and sodium (Na) on the absorbance signal of Se (IV) in 0.5 M acetic acid are given in Figure 3.21, Figure 3.22, Figure 3.23 and Figure 3.24, respectively. Among the all earth-based elements

studied as interfering species, silicon showed the least interfering effect on the signal of selenium as seen in Figure 3.23.

Figueroa and coworkers studied the interference effect of $CaCO_3$ on the signal of selenium. They performed in situ photogeneration of Se volatile compounds to determine Se by ETAAS. It was reported when Se (IV) in acetic acid solution is irradiated at interferent-to-Se concentration ratio of 2000, the recovery of selenium was detected as 87% [71]. However, the results showed that in our study the effect of calcium on selenium signal more compared to that of the study carried by Figueroa and coworkers. As it can be seen from Figure 3.20., calcium did not cause a noticeable effect up to Ca:Se concentration ratio of 50. When this ratio increased to 100, relative Se (IV) signal was measured as 69%. For aluminum, 1:50 of Al:Se concentration ratio caused decreasing the percent relative signal to 66. It is noteworthy that stock solution of Ca from source of $Ca(NO_3)_2$ and stock solution of Al from source of $Al(NO_3)_2$ was used to investigate interferences in this study. It was reported that nitrate (NO_3^-) and nitrite (NO_2^-) ions product of the photoreduction of NO_3^- also influences PVG [75]. It was suggested that nitrate and nitrite ions leads to scavenging of photogenerated free electrons and hydrogen radicals which results in termination of analyte reduction reactions. Thus, nitrate ions in Ca and Al solution could be responsible for the decrease in %relative signal of Se (IV).

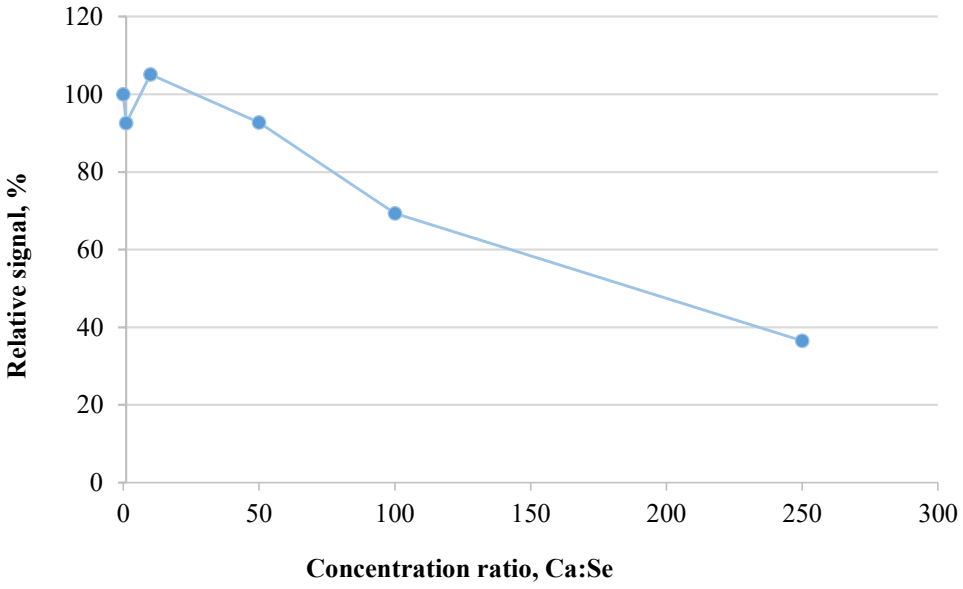

Figure 3.21. Interference effect of calcium on absorbance signal of 50 µg/L Se (IV) in 0.5 M acetic acid. Trapping temperature: 643 ºC, atomization temperature: 1665 ºC argon flow rate: 200 mL/min, hydrogen flow rate: 400 mL/min, trapping volume: 6.0 mL, trapping period: 45 s, sample solution flow rate: 6.0 mL/min.

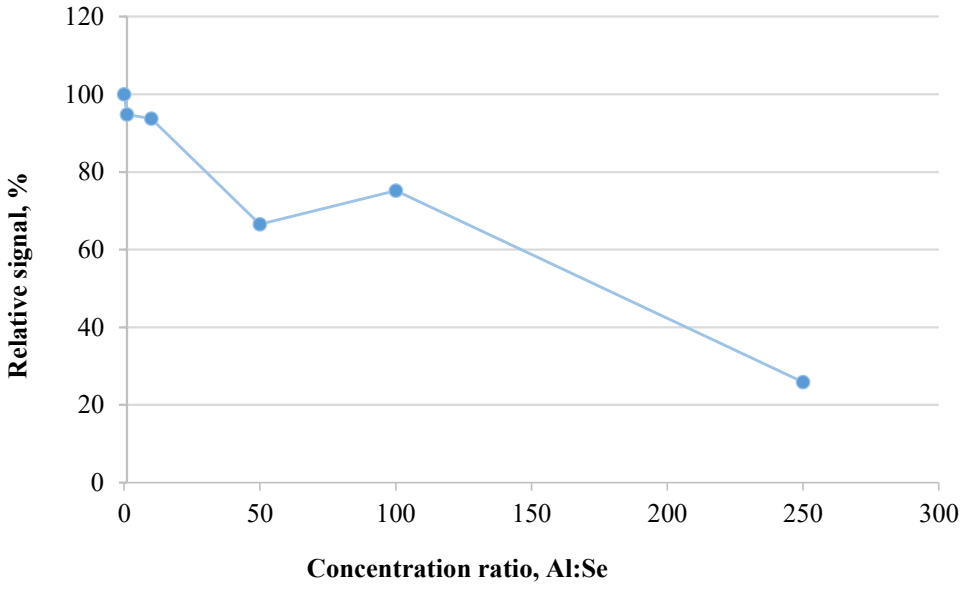

Figure 3.22. Interference effect of aluminum on absorbance signal of 50 µg/L Se (IV) in 0.5 M acetic acid. Trapping temperature: 643 ºC, atomization temperature: 1665 ºC argon flow rate: 200 mL/min, hydrogen flow rate: 400 mL/min, trapping volume: 6.0 mL, trapping period: 45 s, sample solution flow rate: 6.0 mL/min.

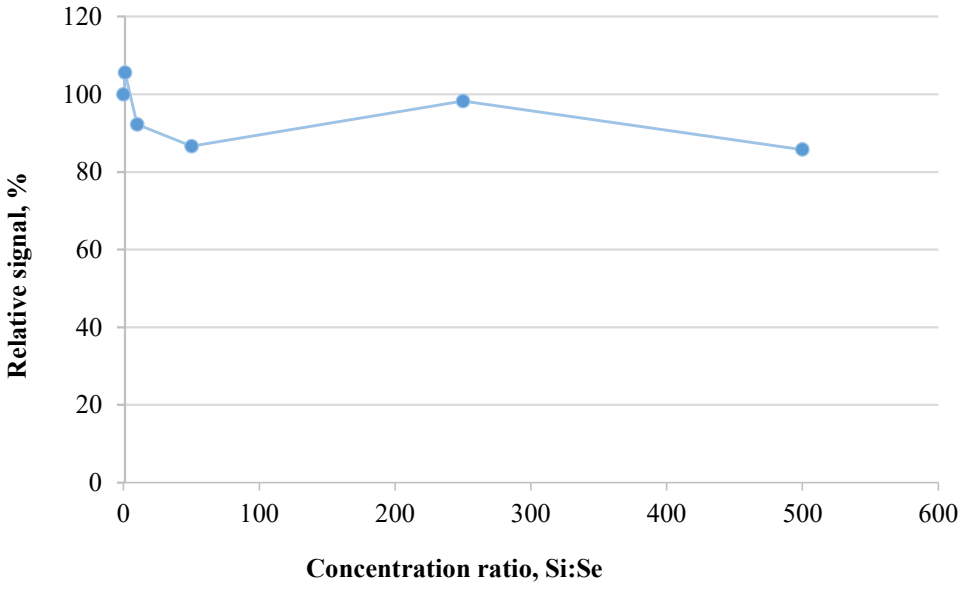

Figure 3.23. Interference effect of silicon on absorbance signal of 50 µg/L Se (IV) in 0.5 M acetic acid. Trapping temperature: 643 ºC, atomization temperature: 1665 ºC argon flow rate: 200 mL/min, hydrogen flow rate: 400 mL/min, trapping volume: 6.0 mL, trapping period: 45 s, sample solution flow rate: 6.0 mL/min.

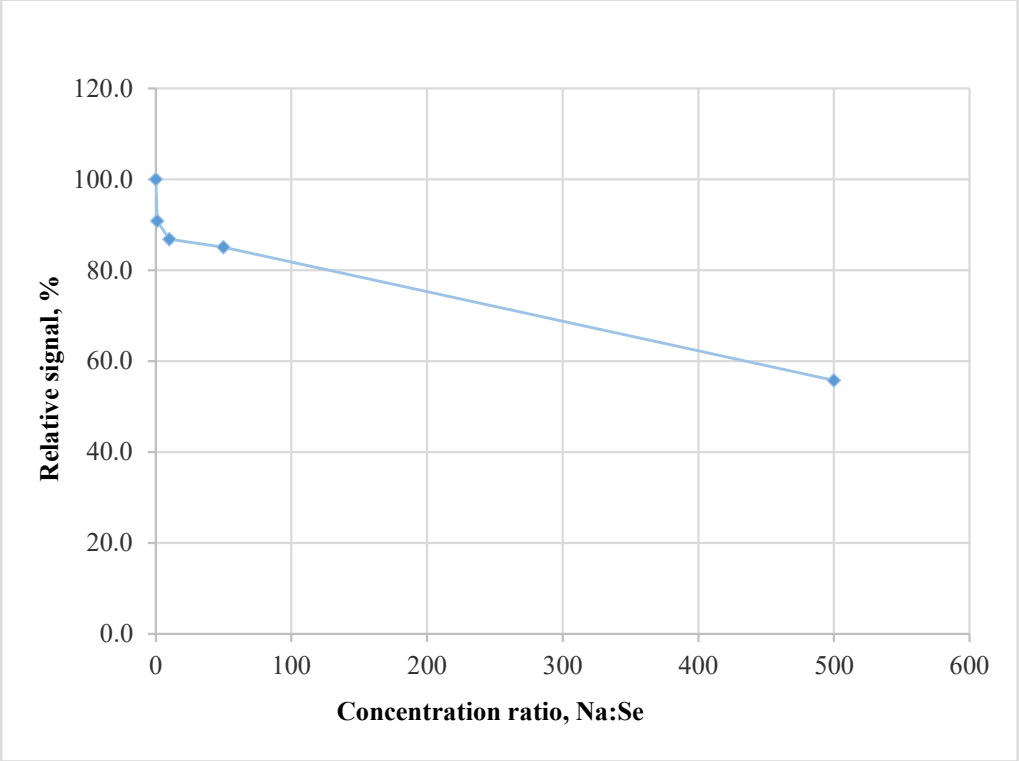

Figure 3.24. Interference effect of sodium on absorbance signal of 50 µg/L Se (IV) in 0.5 M acetic acid. Trapping temperature: 643 ºC, atomization temperature: 1665 ºC argon flow rate: 200 mL/min, hydrogen flow rate: 400 mL/min, trapping volume: 6.0 mL, trapping period: 45 s, sample solution flow rate: 6.0 mL/min.

Similar to silicon, sodium caused tolerable interference on the absorbance signal of Se (IV). As it can be seen from Figure 3.24, interference of sodium on the absorbance signal of Se (IV) was tolerable until the concentration ratio of Na:Se (50:1). However, at higher concentration of sodium, the relative absorbance signal decreased to 55% (concentration ratio of Na:Se 500:1.)

CHAPTER 4

CONCLUSION

Within the scope of this thesis, photochemical vapor generation is coupled to tungsten coil atomizer for the first time in the literature for the determination of selenium.

Selenium was selected as an analyte since its determination in human biology and health is very important. It can be toxic or essential for the human body as well the borderline between these states is sharp. Therefore, detection and quantification of selenium is crucial.

In PVG set-up, major component determining the success of the technique is the UV-photochemical reactor. In this study, it was designed by coiling the FEB tubing around UV lamp. Solutions containing selenium and acetic acid were flowed through this photoreactor. As a result, volatile selenium compounds were generated by UV-light exposure. The technique was combined with tungsten-coil atomization in order to increase sensitivity of photochemical vapor generation system. Generated volatile selenium compounds were trapped and atomized on the tungsten coil.

To obtain reproducible and sharp signals, tungsten coil was coated with different elements having high boiling points. A sharp, most sensitive and reproducible signal was obtained with rhodium coated W-coil.

For the optimization of the technique, following experimental parameters were studied: trapping and atomization temperatures, flow rates of argon and hydrogen gases, concentration of acetic acid, trapping volume, sample flow rate, irradiation time and type of acid. Optimum trapping and atomization temperatures were found as 643 ºC and 1665 ºC, respectively. Optimum argon flow rate was determined as 200 mL/min while optimum hydrogen flow rate was determined as 400 mL/min. Optimization studies of concentration of acetic acid showed that 0.5 mol/L acetic acid

is optimum for the technique. 6.0 mL/min of sample flow rate, 6 mL of trapping volume and 45 s trapping period were other optimized values. Irradiation time of the system was also optimized and 2.5 min was selected to keep the analysis time as short as possible.

Analytical figures of merit of the technique were determined using slope of direct calibration curve and the standart deviation of replicate measurements of blank solution. Linear range of the method was found between 11 and 70 μg/L. LOD and LOQ values of the technique was found to be 3.3 and 11.1 μg/L respectively. LOD value is comparable with the similar studies in literature with PVG technique.

The technique was applied to selenium dietary supplements containing sodium selenite. The concentration of selenium in the tablets was determined by photochemical vapor generation tungsten coil atomization technique. There was no significant difference between the recommended value given by the company and the results obtained from this study.

Interference effect of PVG amenable elements, transition metals and earth-based elements on the PVG signal of selenium was investigated. No significant interference was observed from earth-based elements (Ca, Al and Si). Among the transition metals studied, the most severe interference was observed with Cu compared to Mn and Ni. PVG amenable elements (Sb, Pb) also showed significant interference on the absorbance signal of selenium.

To conclude, photochemical vapor generation coupled to tungsten coil atomization technique was applied successfully for the determination of Se (IV). Although analytical figures of merit were not very competitive, simplicity and cost effectiveness of W-coil atomizer are advantageous of this method.

REFERENCES

1. Reilly C. *Selenium in Food and Health*. 2nd ed. Brisbane, Australia; 2006. doi:10.1007/978-0-387-33244-4

2. Terry EN, Diamond AM. Selenium. 2012;(1973):568-585.

3. Fan AM, Vinceti M. *Hamilton & Hardy's Industrial Toxicology*. Vol 134.; 2015.

4. Chen YW, Li L, D'Ulivo A, Belzile N. Extraction and determination of elemental selenium in sediments-A comparative study. *Anal Chim Acta*. 2006;577(1):126-133. doi:10.1016/j.aca.2006.06.020

5. Alexander J. *Selenium*. Vol 1.; 2014. doi:10.1016/B978-0-444-59453-2.00052-4

6. Jorgenson BJD. Selenium and tellurium. *US Geol Surv Miner Yearb*. 2002:1-7.

7. Oopmann DK, Ag B, Republic F. Selenium and selenium compounds. *IARC Monogr Eval Carcinog Risk Chem Man*. 1975;9(112945):245-260. doi:10.1002/14356007.a23

8. World Health Organization. Trace elements in human nutrition and health World Health Organization. *World Heal Organ*. 1996:1-360. https://apps.who.int/iris/bitstream/handle/10665/37931/9241561734_eng.pdf.

9. Combs GF. Selenium in global food systems. *Br J Nutr*. 2001;85(05):517. doi:10.1079/BJN2000280

10. Mehdi Y, Hornick JL, Istasse L, Dufrasne I. Selenium in the environment, metabolism and involvement in body functions. *Molecules*. 2013;18(3):3292-3311. doi:10.3390/molecules18033292

11. Crews, H.M., Lewis D.J., Fairweather-Tait S.J., Fox T. The analyst's viewpoint

with special reference to selenium. *Nutr Food Sci*. 1997;97(6):221-224. doi:10.1108/00346659710180334

12. Welz B, Sperling M. *Atomic Absorption Spectrometry*. 3rd ed. Weinheim; 2005.

13. Dale IM. Atomic Absorption Spectrometry. *Tech Instrum Anal Chem*. 1982;5:381-394. doi:10.1016/S0167-9244(08)70094-5

14. Moldovan M. *Atomic Absorption Spectrometry—Flame*. Elsevier Inc.; 2013. doi:10.1016/b978-0-12-409547-2.00022-6

15. Cantle JE. *Atomic Absorption Spectrometry*. (Cantle JE, ed.). New York: Elsevier Scientific Publishing Company; 1982.

16. Farey BJ, Nelson LA. Atomic absorption spectrometry. *Tech Instrum Anal Chem*. 1982;5:67-94. doi:10.1016/S0167-9244(08)70083-0

17. Lajunen LHJ, Peramaki P. *Spectrochemical Analysis by Atomic Absorption and Emission*.; 2004. doi:10.1039/9781847551900

18. Yan X-P, Ni Z-M. Vapour generation atomic absorption spectrometry. *Anal Chim Acta*. 1994;291(1-2):89-105. doi:10.1016/0003-2670(94)85130-1

19. de Souza SS, Santos D, Krug FJ, Barbosa F. Exploiting in situ hydride trapping in tungsten coil atomizer for Se and As determination in biological and water samples. *Talanta*. 2007;73(3):451-457. doi:10.1016/j.talanta.2007.04.031

20. Sturgeon RE, Mester Z. Analytical applications of volatile metal derivatives. *Appl Spectrosc*. 2002;56(8). doi:10.1366/000370202760249675

21. D'Ulivo A, Mester Z, Sturgeon RE. The mechanism of formation of volatile hydrides by tetrahydroborate(III) derivatization: A mass spectrometric study performed with deuterium labeled reagents. *Spectrochim Acta - Part B At Spectrosc*. 2005;60(4):423-438. doi:10.1016/j.sab.2005.03.015

22. Wypych G. Photophysics. In: *Handbook of Material Weathering*. ; 2018:1-26. doi:10.1016/B978-1-927885-31-4.50003-0

23. Nakazato T, Tao H. A high-efficiency photooxidation reactor for speciation of organic arsenicals by liquid chromatography-hydride generation-ICPMS. *Anal Chem*. 2006;78(5):1665-1672. doi:10.1021/ac051783f

24. Sturgeon RE. Photochemical vapor generation: A radical approach to analyte introduction for atomic spectrometry. *J Anal At Spectrom*. 2017;32(12):2319-2340. doi:10.1039/c7ja00285h

25. Kikuchi E, Sakamoto H. Kinetics of the reduction reaction of selenate ions by TiO2 photocatalyst. *J Electrochem Soc*. 2002;147(12):4589. doi:10.1149/1.1394106

26. Guo X, Sturgeon RE, Mester Z, Gardner GJ. UV light-mediated alkylation of inorganic selenium. *Appl Organomet Chem*. 2003;17(8):575-579. doi:10.1002/aoc.473

27. Guo X, Sturgeon RE, Mester Z, Gardner GJ. UV vapor generation for determination of selenium by heated quartz tube atomic absorption spectrometry. *Anal Chem*. 2003;75(9):2092-2099. doi:10.1021/ac020695h

28. Zheng C, Li Y, He Y, Ma Q, Hou X. Photo-induced chemical vapor generation with formic acid for ultrasensitive atomic fluorescence spectrometric determination of mercury: Potential application to mercury speciation in water. *J Anal At Spectrom*. 2005;20(8):746-750. doi:10.1039/b503727a

29. Yin YG, Liu JF, He B, Gao E Le, Jiang G Bin. Photo-induced chemical vapour generation with formic acid: Novel interface for high performance liquid chromatography-atomic fluorescence spectrometry hyphenated system and application in speciation of mercury. *J Anal At Spectrom*. 2007;22(7):822-826. doi:10.1039/b701514c

30. Campanella B, Menciassi A, Onor M, Ferrari C, Bramanti E, D'Ulivo A.

Studies on photochemical vapor generation of selenium with germicidal low power ultraviolet mercury lamp. *Spectrochim Acta - Part B At Spectrosc*. 2016;126:11-16. doi:10.1016/j.sab.2016.10.007

31. Guo X, Sturgeon RE, Mester Z, Gardner GJ. Photochemical alkylation of inorganic arsenic : Part 1. Identification of volatile arsenic species. *J Anal At Spectrom*. 2005;20(8):702. doi:10.1039/b503661e

32. McSheehy S, Guo XM, Sturgeon RE, Mester Z. Photochemical alkylation of inorganic arsenic Part 2. Identification of aqueous phase organoarsenic species using multidimensional liquid chromatography and electrospray mass spectrometry. *J Anal At Spectrom*. 2005;20(8):709-716. doi:10.1039/b503662c

33. Grinberg P, Sturgeon RE. Photochemical vapor generation of iodine for detection by ICP-MS. *J Anal At Spectrom*. 2009;24(4):508-514. doi:10.1039/b814272f

34. Sturgeon RE. Detection of bromine by ICP- oa -ToF-MS following photochemical vapor generation. *Anal Chem*. 2015;87(5):3072-3079. doi:10.1021/ac504747a

35. Guo X, Sturgeon RE, Mester Z, Gardner G. UV photosynthesis of nickel carbonyl. *Appl Organomet Chem*. 2004;18(5):205-211. doi:10.1002/aoc.602

36. Grinberg P, Sturgeon RE, Gardner G. Identification of volatile iron species generated by UV photolysis. *Microchem J*. 2012;105:44-47. doi:10.1016/j.microc.2012.05.036

37. Grinberg P, Mester Z, Sturgeon RE, Ferretti A. Generation of volatile cobalt species by UV photoreduction and their tentative identification. *J Anal At Spectrom*. 2008;23(4):583-587. doi:10.1039/b717216h

38. Sturgeon RE, Grinberg P. Some speculations on the mechanisms of photochemical vapor generation. *J Anal At Spectrom*. 2012;27(2):222. doi:10.1039/c2ja10249h

39. Takatani T, Fitzgerald N, Galbraith JM. Proposed reaction mechanisms for selenium UV photolysis vapor generation by computational methods. *Anal Bioanal Chem*. 2007;388(4):859-862. doi:10.1007/s00216-006-0742-5

40. Zheng C, Wu L, Ma Q, Lv Y, Hou X. Temperature and nano-TiO2 controlled photochemical vapor generation for inorganic selenium speciation analysis by AFS or ICP-MS without chromatographic separation. *J Anal At Spectrom*. 2008;23:514. doi:10.1039/b713651j

41. Yang W, Gao Y, Wu L, Hou X, Zheng C, Zhu X. Preconcentration and in-situ photoreduction of trace selenium using TiO2 nanoparticles, followed by its determination by slurry photochemical vapor generation atomic fluorescence spectrometry. *Microchim Acta*. 2014;181(1-2):197-204. doi:10.1007/s00604-013-1101-9

42. Rybínová M, Erven V, Rychlovsk P. UV-photochemical vapour generation with in situ trapping in a graphite tube atomizer for ultratrace determination of selenium. *J Anal At Spectrom*. 2015;30(8):1752-1763. doi:10.1039/C5JA00173K

43. Rybínová M, Červený V, Hraníček J, Rychlovský P. UV-photochemical vapor generation with quartz furnace atomic absorption spectrometry for simple and sensitive determination of selenium in dietary supplements. *Microchem J*. 2016;124:584-593. doi:10.1016/j.microc.2015.10.004

44. Rybínová M, Musil S, Červený V, Vobecký M, Rychlovský P. UV-photochemical vapor generation of selenium for atomic absorption spectrometry: Optimization and 75Se radiotracer efficiency study. *Spectrochim Acta - Part B At Spectrosc*. 2016;123:134-142. doi:10.1016/j.sab.2016.08.009

45. Republic C. Atomization of volatile compounds for atomic absorption and atomic fluorescence spectrometry : On the way towards the ideal atomizer ☆. 2007;62(November 2006):846-872. doi:10.1016/j.sab.2007.05.002

46. Academy C. Hydride atomization in a cool hydrogen-oxygen burning in a quartz tube atomizer covalent hydrides such as Se , Te , As , Sb , etc ., are often determined absorption spectrometry . Atomization in a diffusion argon-hydrogen flame which was either in the fla. 1980;35(1975):119-128.

47. Dedina J, Welz B. Quartz tube atomisers for hydride generation atomic absorption spectrometry: mechanism for the atomisation of arsine. *J Anal At Spectrom*. 1992;7(March):307-314.

48. Hou X, Jones BT. Tungsten devices in analytical atomic spectrometry. *Spectrochim Acta - Part B At Spectrosc*. 2002;57(4):659-688. doi:10.1016/S0584-8547(02)00014-9

49. Lide DR et al. CRC Handbook of Chemistry and Physics, Internet Version 2005. *J Am Chem Soc*. 2005:2661. doi:10.1021/ja906434c

50. Barbosa Jr F, Simiao de Souza S, Krug FJ. In situ trapping of selenium hydride in rhodium-coated tungsten coil electrothermal atomic absorption spectrometry. *J Anal At Spectrom*. 2002;17(4):382-388. doi:10.1039/B111129A

51. Hou X, Yang Z, Jones BT. Determination of selenium by tungsten coil atomic absorption spectrometry using iridium as a permanent chemical modifier. *Spectrochim Acta - Part B At Spectrosc*. 2001;56(2):203-214. doi:10.1016/S0584-8547(00)00305-0

52. Ataman OY. Vapor generation and atom traps: Atomic absorption spectrometry at the ng/L level. *Spectrochim Acta - Part B At Spectrosc*. 2008;63(8):825-834. doi:10.1016/j.sab.2008.03.013

53. Watling RJ. The Use of a Slotted Quartz Tube For The Analysis of Trace Metals in Fresh Water. 1977;3(4):218-221.

54. Watling RJ. The use of a slotted quartz tube for the determination of arsenic, antimony, selenium and mercury. *Anal Chim Acta*. 1977;94(1):181-186.

doi:10.1016/s0003-2670(01)83645-x

55. Watling RJ. The use of a slotted tube for the determination of lead, zinc, cadmium, bismuth, cobalt, manganese and silver by atomic absorption spectrometry. *Anal Chim Acta*. 1978;97:395-398. http://staff.najah.edu/sites/default/files/short-communication-synthesis-and-dethiation-5-phenyl-3-thioxo-23-dihydro-1h-24-benzodiazepine-1-on.pdf.

56. Thorburn Burns D, Chimpalee N, Harriott M. Applications of a slotted tube atom trap and flame atomic absorption spectrometry: Determination of tin in copper-based alloys after hydride generation. *Fresenius J Anal Chem*. 1994;349(7):530-532. doi:10.1007/BF00323988

57. Thorburn Burns D, Chimpalee N, Harriott M. Applications of a slotted tube atom trap and flame atomic absorption spectrometry: Determination of bismuth in copper-based alloys with and without hydride generation. *Fresenius J Anal Chem*. 1995;311:93-97. doi:10.1007/BF00323988

58. Ataman OY. Economical Alternatives for High Sensitivity in Atomic Spectrometry Laboratory. *Pakistan J Anal Environ Chem*. 2007;8(1):64-68.

59. Ertas N, Korkmaz DK, Kumser S, Ataman OY. Novel traps and atomization techniques for flame AAS. 2002:1415-1420. doi:10.1039/b206363h

60. Karadeniz Korkmaz D, Ertaş N, Ataman OY. A novel silica trap for lead determination by hydride generation atomic absorption spectrometry. *Spectrochim Acta - Part B At Spectrosc*. 2002;57(3):571-580. doi:10.1016/S0584-8547(01)00379-2

61. Cankur O, Ertas N, Ataman OY. Determination of bismuth using on-line preconcentration by trapping on resistively heated W coil and hydride generation atomic absorption spectrometry. *J Anal At Spectrom*. 2002;17:603-609. doi:10.1039/b201365g

62. Dever JA, Pietromica AJ, Park B, et al. Simulated Space Vacuum Ultraviolet

(VUV) Exposure Testing for Polymer Films. *Sci York*. 2001;(January).

63. Jiri Dedina DLT. *Hydride Generation Atomic Absorption Spectrometry*. John Wiley & Sons Inc, United States; 1995.

64. Bora S. Simultaneous Determination of Bismuth and Tellurium Using Tungsten Coil Atom Trap with Inductively Coupled Plasma Mass Spectrometry. 2016;(January).

65. Njie N. Atom Trapping Vapor Generaton Atomic Absorption Spectrometry for Inorganic Arsenic Speciation Analysis. 2014.

66. Silva SG, Donati GL, Santos LN, Jones BT, Nóbrega JA. Cobalt as chemical modifier to improve chromium sensitivity and minimize matrix effects in tungsten coil atomic emission spectrometry. *Anal Chim Acta*. 2013;780:7-12. doi:10.1016/j.aca.2013.04.006

67. Virgilio A, Nóbrega JA, Jones BT, Donati GL. Chemical modification in atomic emission: Determination of V in lubricant oils by tungsten coil atomic emission spectrometry. *Microchem J*. 2014;115:58-62. doi:10.1016/j.microc.2014.02.011

68. Parsons PJ, Qiao H, Aldous KM, Mills E, Slavin W. A low-cost tungsten filament atomizer for measuring lead in blood by atomic absorption spectrometry. *Spectrochim Acta Part B At Spectrosc*. 1995;50(12):1475-1480. doi:10.1016/0584-8547(95)01416-0

69. Bruhn CG, San Francisco NA, Neira JY, Nóbrega JA. Determination of cadmium and lead in mussels by tungsten coil electrothermal atomic absorption spectrometry. *Talanta*. 1999;50(5):967-975. doi:10.1016/S0039-9140(99)00186-1

70. Zhou Y, Parsons PJ, Aldous KM, Brockman P, Slavin W. Atomization of lead from whole blood using novel tungsten filaments in electrothermal atomic absorption spectrometry. *J Anal At Spectrom*. 2001;16(1):82-89.

doi:10.1039/b006644n

71. Figueroa R, García M, Lavilla I, Bendicho C. Photoassisted vapor generation in the presence of organic acids for ultrasensitive determination of Se by electrothermal-atomic absorption spectrometry following headspace single-drop microextraction. *Spectrochim Acta - Part B At Spectrosc*. 2005;60(12):1556-1563. doi:10.1016/j.sab.2005.10.009

72. Dědina J. Interference of Volatile Hydride Forming Elements in Selenium Determination by Atomic Absorption Spectrometry with Hydride Generation. *Anal Chem*. 1982;54(12):2097-2102. doi:10.1021/ac00249a043

73. Duan H, Zhang N, Gong Z, Li W, Hang W. Photochemical vapor generation of lead for inductively coupled plasma mass spectrometric detection. *Spectrochim Acta - Part B At Spectrosc*. 2016;120:63-68. doi:10.1016/j.sab.2016.04.003

74. Bideau M, Claudel B, Faure L, Rachimoellah M. Homogeneous and heterogeneous photoreactions of decomposition and oxidation of carboxylic acids. *J Photochem*. 1987;39(1):107-128. doi:10.1016/0047-2670(87)80010-2

75. Lopes GS, Sturgeon RE, Grinberg P, Pagliano E. Evaluation of approaches to the abatement of nitrate interference with photochemical vapor generation. *J Anal At Spectrom*. 2017;32(12):2378-2390. doi:10.1039/c7ja00311k